Retardation of oil cracking to gas and pressure induced combination reactions to account for viscous oil in deep petroleum basins: Evidence from oil and *n*-hexadecane pyrolysis at water pressures up to 900 bar

Clement N. Uguna [a,c*], Andrew D. Carr [b], Colin E. Snape [a], Will Meredith [a]

[a] *Faculty of Engineering, University of Nottingham, The Energy Technologies Building, Innovation Park, Jubilee Campus, Triumph Road, Nottingham, NG7 2TU, UK.*

[b] *Advanced Geochemical Systems Ltd., 1 Towles Fields, Burton-on-the-Wolds, Leicestershire, LE12 5TD, UK.*

[c] *Centre for Environmental Geochemistry, British Geological Survey, Keyworth, Nottingham, NG12 5GG, UK.*

*Corresponding author: clement.uguna@nottingham.ac.uk; uguna@bgs.ac.uk; Tel: 44 (0)115 748 4458

Abstract

This study reports a laboratory pyrolysis experimental study on oil and *n*-hexadecane to rationalise the thermal stability of oil in deep petroleum reservoirs. Using a 25 ml Hastalloy pressure vessel, a 35° API North Sea oil (Oseberg) and *n*-hexadecane (*n*-C_{16}), were pyrolysed separately under non-hydrous (20 bar), low pressure hydrous (175 bar) and high liquid water pressure (500 and 900 bar) at 350 °C for 24 h. This study shows that the initial cracking of oil and *n*-hexadecane to hydrocarbon gases was retarded in the presence of water (175 bar hydrous conditions) compared to low pressures in the absence of water (non-hydrous conditions). At 900 bar water pressure, the retardation of oil and *n*-hexadecane cracking was more significant compared to 175 bar hydrous and 500 bar water pressure conditions. Combination reactions have been observed for the first time in pressurised water experiments during the initial stages of cracking, resulting in the increased abundance of heavier *n*-alkane hydrocarbons (>C_{20}), the amount of unresolved complex material (UCM), as well as the asphaltene content of the oil. These reactions, favoured by increasing water pressure provide a new mechanism for rationalising the thermal stability of oils, and for producing heavy oils at temperatures above which biodegradation can occur. Indeed, we demonstrate that bitumen from the high pressure Gulf of Mexico basin has been formed from lighter oil components and it possesses similar characteristics to the laboratory oils generated.

Keywords: Oil cracking, *n*-hexadecane cracking, oil viscosity, high water pressure, pressure retardation, combination reactions.

1. Introduction

The thermal cracking of petroleum and its conversion into gas and pyrobitumen in geological basins appears to occur between 150 and 200 °C, and has been the subject of extensive investigations using field data (e.g. Price et al., 1979; Price et al., 1981; Price, 1982; Mango, 1991; Hayes, 1991), laboratory pyrolysis investigation of oils (e.g. Ungerer and Pelet, 1987; Ungerer et al., 1988; Behar et al., 1992; Behar et al., 1997a; 1997b; Schenk et al., 1997; Dieckmann et al., 1998; Lewan and Ruble, 2002; Hill et al., 2003; Lehne and Dieckmann, 2007a; 2007b; Behar et al., 2008), or theoretical calculations (e.g. Dominé et al., 1998). Undegraded crude oils generally show an increase in both API gravity and gas to oil ratio (GOR) with increasing depth of burial (Tissot and Welte, 1984), which can result from the conversion of oil into lighter hydrogen-rich products (gas and condensate) and heavy carbon rich solid residues (coke or pyrobitumen). Pyrobitumen forms either by aromatic condensation reactions (Ungerer et al., 1988; Behar et al., 1992), or directly from nitrogen sulphur and oxygen (NSO) compounds (Hill et al., 2003). Oil cracking to gas was described as occurring via hydrogen transfer reactions (Bailey et al., 1974; Connan et al., 1975), although it also appears that the mechanism involves free radical reactions (Rice and-Herzfeld 1934), with initiation, hydrogen transfer, decomposition of carbon-carbon bonds by ß-scission, radical isomerization, addition and termination processes in the oil (e.g. Bounaceur et al. 2002a; Burkle-Vitzthum et al., 2004).

In addition to actual oils, numerous studies have also been conducted using individual aliphatic hydrocarbons between *n*-hexane and *n*-hexadecane to investigate the thermal cracking of oil (e.g. Fabuss et al., 1964; Ford, 1986; Dominé, 1989; 1991;

Khorasheh and Gray, 1993a; 1993b; Song et al., 1994; Jackson et al., 1995; Behar and Vandenbroucke, 1996). The thermal cracking of aliphatic hydrocarbons involves their conversion into lower molecular weight alkanes and alkenes, and with minor yields of aromatic compounds (Rice, 1931; 1933; Voge and Good, 1949; Ford, 1986; Zhou et al., 1987; Bounaceur et al., 2002a) together with branched alkanes of higher molecular weight than the starting alkane. Experimental observations show that the concentration of alkenes decrease with increasing conversion, while the alkanes increase in concentration, especially those with a higher number of carbon atoms than the reactant (Khorasheh and Gray, 1993a; Ford, 1986; Dominé, 1989; Dominé et al., 1990).

The cracking of aromatic compounds has been investigated (Savage and Klein, 1987; Freund and Olsmtead, 1989; Poutsma, 1990; Smith and Savage, 1991; 1994; Burnham et al., 1998; Yu and Eser, 1998; Behar et al., 1999; 2002; Bounaceur et al., 2000; Burklé-Vitzthum et al., 2003; 2004; 2005; Dartiguelongue et al., 2006; Leininger et al., 2006). The thermal stability of alkylaromatics depends on the number of aromatic rings and length of the side chain (Smith and Savage, 1991; Behar et al., 2002). The main degradation products appear to be a combination of heavy aromatics (e.g. phananthrenes), lighter aromatics (e.g. naphthalene, toluene), alkanes and gases (Behar et al., 2002). The effect of co-reactions between aromatics and hydrocarbon mixtures in laboratory pyrolysis was studied by Burkle-Vitzthum et al. (2004; 2005) and by Lannuzel et al. (2010). Benzene does not have any kinetic effect on the thermal cracking of alkanes (Burkle-Vitzthum et al., 2004), although addition reactions with methyl radicals leads to the formation of toluene, and depending on the temperature and pressure conditions, toluene is potentially a strong inhibitor of *n*-alkanes cracking (Burkle-Vitzthum et al., 2004; 2005; Lannuzel et al., 2010). The inhibition of *n*-alkane

84 cracking by monoaromatics, e.g. alkylbenzenes, tertralin, hydronaphthalenics, has also
85 been widely observed (e.g. Behar et al., 2002; Bounaceur et al., 2002b; Burkle-
86 Vitzthum et al., 2005; Burnham et al., 1997; McKinney et al., 1998). The composition
87 of oils in subsurface reservoirs in geological basins ranges between heavy oils with
88 relatively low alkane-aromatic ratios, to light, condensates with high alkane-aromatic
89 ratios, means that there are many potential interactions between the different
90 components depending on the temperature and pressure histories of the reservoir.

91 While much of the work on the stability of hydrocarbons has concentrated on the
92 stability with temperature, the other physical factor that needs to be considered is
93 pressure. Given that the oil to gas process results in a volume increase (Barker, 1990),
94 then such changes should be controlled by the system temperature and pressure. The
95 influence of pressure has not received as much attention as that devoted to temperature.
96 It is important to recognise that the experimental design used to simulate the effects of
97 pressure need to be assessed. In most of the experiments undertaken up to this point,
98 the experiments investigating the effects of pressure have used gold-bags (confined
99 pyrolysis), in which the sample (oil or model compound) is sealed within a gold-bag
100 (having removed vapour from inside the gold-bag prior to sealing), and the gold-bag is
101 then inserted within a vessel in which pressure is applied to the external surface of the
102 gold-bag. The important point is that the oil or model compounds being pyrolysed are
103 not in contact with the water. Most of the work on the effect of pressure has been
104 undertaken on model compounds, e.g. saturates and aromatics, although Hill et al.
105 (1996) pyrolysed the C_9+ fraction of a saturate-rich, West Canadian Devonian oil in
106 sealed gold tubes at temperatures between 350 and 400 °C for 72 h and at pressures
107 between 90 and 2000 bar, and found that the effect of pressure on the rate of oil

cracking and product generation was small. In a number of studies, a retardation effect was observed during the pyrolysis of saturated hydrocarbons at pressures higher than 400 bar (Fabuss et al., 1964; Dominé, 1991; Behar and Vandenbroucke, 1996). At lower pressures, Fabuss et al. (1964) concluded that pressure accelerates cracking between 1 and 400 bar while a decrease was observed at higher pressure (800 bar). This trend of an initial increase followed by a decrease at higher pressure has been confirmed for oil cracking (Behar and Vandenbroucke, 1996; Hill et al., 1996). On the contrary, Jackson et al. (1995) observed a continuous retarding effect for *n*-hexadecane pyrolysis between 120 and 600 bar. Al Darouich et al. (2006) (using the light aromatic fraction of a crude oil pyrolysed at 375 °C under pressures of 400, 800 and 1200 bar) showed that a pressure increase from 100 to 400 bar reduced the cracking of light aromatic fractions, unstable charge-classes, and secondary cracking of the C_{15}–C_{20} and C_{20+} compounds, which reduced the production of gas and insoluble residue. However further increase in pressure produced only minor changes compared with those produced by increasing the pressure from 100 to 400 bar.

Unlike the confined pyrolysis non-hydrous studies reported above, water is present in most rocks in geological basins, even if only as the irreducible water saturating hydrocarbon reservoirs. Although source rocks have been pyrolysed in the presence of water (hydrous pyrolysis), relatively few studies have been undertaken using water and oil in the pyrolysis experiment. It must be recognised that in addition to the presence of liquid water and not steam, other factors such as the physical state of the water as the solubility of hydrocarbons in water depends strongly on water phase state, and the chemical effect of the water need to be considered. Some work on the effect of water on the stability of hydrocarbons has been undertaken, Abbott et al.

(1995) showed that 5α(H)-cholestane was more degraded under anhydrous compared to hydrous conditions. Hydrous pyrolysis experiments on a Japanese oil derived from a type II source rock by Tsuzuki et al. (1999) showed that the cracking reaction rates were retarded compared with non-hydrous experiments. Brooks et al. (1971) as well as Hesp and Rigby (1973) also showed that the pyrolysis of oil in the presence of water and under inert gas pressure retarded oil to gas cracking reactions compared with non-hydrous and absence of pressure, while oil cracking to gas was retarded between 700 and 900 bar water pressure for coal pyrolysed at 420 °C for 24 h (Uguna et al., 2015). In an attempt to evaluate the role of water, Hoering (1984) undertook a series of hydrous pyrolysis experiments with pulverized rock, model compounds, and D_2O. This study demonstrated deuterium exchanged with hydrogen in hydrocarbons that were cleaved from decomposing kerogen, but the specific role of water in the pyrolysis reactions and its ability to promote oil expulsion from an organic-rich rock was not determined. The objective of the Hoering (1984) study was to address this uncertainty through a series of experiments designed to evaluate various roles water may play in petroleum formation. Although this study uses petroleum rather than kerogen, similar processes involving the cleavage of carbon-carbon bonds in free radical reactions in petroleum as opposed to kerogen can be expected to occur.

The studies by Brooks et al. (1971) and Hesp and Rigby (1973) used a maximum pressure of 210 atm. (213 bar equivalent to hydrostatic pressure at 2.4 km) at 375 °C under hydrous conditions. Although oil cracking was retarded in the presence of water, the effect that the increase in pressure has on oil cracking was not fully investigated, as temperature was only the parameter varied in their experiment. In our previous studies, we have investigated gas and oil generation, and oil cracking from

156 petroleum source rocks and coal under high water pressure conditions. The aim of this
157 study is to take further the earlier findings by Brooks et al. (1971) as well as Hesp and
158 Rigby (1973) that oil cracking to gas was retarded in the presence of water by
159 comparing the effect of increased water pressure on the cracking of expelled oil in deep
160 water petroleum saturated reservoirs. It presents results for laboratory pyrolysis
161 experiments conducted on a 35° API North Sea oil and *n*-hexadecane (*n*-C_{16}) at 350 °C
162 under non-hydrous low pressure conditions (20 bar), normal hydrous pressure (175 bar),
163 and high water pressure (500 and 900 bar) conditions for 24 h. The aim of this study is
164 also to investigate the gross changes in oil quality expected to occur as they are buried
165 to greater depths and higher temperatures and pressures after emplacement in a
166 reservoir. Having investigated the effect of water pressure on oil generation and
167 expulsion from the Kimmeridge Clay (Uguna et al., 2016) which is the equivalent of
168 Draupne source rock that generated the Oseberg oil in the Norwegian North Sea (Dahl
169 and Speers, 1985), the oil was chosen to investigate the potential cracking of oil to gas.
170 Given the preliminary nature of this work, no attempt has been made to understand the
171 mechanisms involved. However, at high pressures, bimolecular reactions (radical
172 addition and hydrogen abstraction) are favoured over the unimolecular radical
173 decomposition (Khorasheh and Gray, 1993a) which also have higher activation energies
174 than bimolecular reactions and are favoured at higher temperatures. The physical effect
175 played by the virtual incompressible nature of high-pressure water has never been
176 investigated for oil cracking, but it would be expected to play an important role due to
177 the effect that it has on the reaction kinetics. As the pressure increases, for endothermic
178 volumetric expansion reactions, such as cracking, the amount of energy required to
179 achieve the activated complex increases, due to the increased positive pV work

component of the activation energy. In contrast for exothermic, e.g. combination, reactions the pV work is subtracted from the activation energy, and thus high pressure favours such reactions. This is also likely to arise from the pre-exponential A factor increasing due to the higher collision rates between reacting species.

When considering the results from laboratory experiments under 175 bar hydrous, 500 and 900 bar water pressures as reported in this study, it is always important to compare the laboratory conditions to those present in geological basins. In this study the temperature of 350 °C is far higher than the temperatures at which oil is found in geological reservoirs, while pressures of 175 bar, 500 bar and 900 bar are the hydrostatic pressures at 1.7 km, 5 km and 9 km respectively, assuming no overpressure in all cases. The pyrolysed oil was also compared to a Gulf of Mexico (GOM) bitumen sample from a depth of 20,353 ft. and reservoir pressure of 822 bar. The GOM bitumen used here was not a solvent soluble bitumen fraction of a source rock, but a tar like solid bitumen (containing gasoline range hydrocarbons) soluble in dichloromethane. This bitumen was chosen because of the depth and reservoir pressure it was obtained from to compare it to the oil residue after pyrolysis, and to further investigate if the bitumen was formed from oil cracking. The GOM bitumen and its asphaltene were analysed by gas chromatography (GC), gas chromatography-mass spectrometry (GC-MS) and hydropyrolysis (HyPy). Hydropyrolysis is an open-system continuous flow pyrolysis technique, which in the presence of a molybdenum catalyst and high hydrogen gas pressures (15 MPa) possesses the unique ability to produce high yields of hydrocarbon biomarkers from source rock kerogens and petroleum asphaltenes, whilst minimising structural alteration by isomerisation and cracking. The hopane and sterane biomarkers covalently bound within the macromolecular structure of the asphaltenes and released

by HyPy, are found to undergo the same epimerisation reaction pathways as their free counterparts in the maltene fraction. They are however for most oils generally less mature then the free biomarkers in terms of isomerisation at both ring and side-chain chiral centres (Murray et al., 1998; Russell et al., 2004).

2. Experimental

2.1. Pyrolysis experiments

Pyrolysis experiments were conducted using 1.2 g of *n*-hexadecane and 2.0 g of oil at 350 °C (temperature accuracy ±1 °C) for 24 h under non-hydrous (no water added), low pressure hydrous (175 bar) and high liquid water pressure (500 and 900 bar) pyrolysis conditions. The *n*-hexadecane and oil pyrolysis experiments were performed separately using the same pyrolysis equipment and experimental procedure that has been published previously (Uguna et al., 2012a; 2015) and also described here. The pyrolysis equipment (Figure 1) comprised a Hastalloy (25 ml cylindrical) pressure vessel (rated to 1400 bar at 420 °C, designed by Strata Technology, Sunbury-on-Thames, UK) connected to an Autoclave Engineers pressure gauge and rupture disc rated to 950 bar. Heat was applied by means of a fluidised sand bath, controlled by an external temperature controller. Temperature was also monitored independently by means of a K-Type thermocouple attached to the outside of the vessel and recorded by computer every 10 seconds. The low pressure hydrous experiments were conducted with the addition of 15 ml distilled water to the vessel, generating a pressure of 175 bar. The oil or *n*-hexadecane to be pyrolysed was directly weighed into the empty vessel, after which 12 g of pre-extracted glass beads (80 mesh particle size) was added to the vessel before the volume of water needed for the experiment was added. It is

227 noteworthy here that the reaction product distributions during the hydrous pyrolysis of a
228 sterane model compound were very similar in a comparison of the reactions carried out
229 in stainless steel-316 and borosilicate glass reactors (Abbott et al., 1995). Glass beads
230 were to adsorb the oil or *n*-hexadecane to ensure the samples were submerged in water
231 during the 175, 500 and 900 bar experiments. For all experiments, the reaction vessel
232 was flushed with nitrogen gas to replace air in the reactor head space, after which 2 bar
233 pressure of nitrogen was pumped into the pressure vessel to produce an inert
234 atmosphere during the pyrolysis runs. The sand bath (connected to a compressed air
235 source) was pre-heated to the required experimental temperature (350 °C) and left to
236 equilibrate, after which the pressure vessel was then lowered into the sand bath and the
237 experiment left to run with a constant air flow through the sand bath. The pressure
238 observed for the low pressure (175 bar) experiment was generated by the vapour of the
239 water (15 ml) added to the vessel at the start of the experiment.

240 High liquid water pressure (500 and 900 bar) experiments were performed
241 similarly to the low (175 bar) pressure hydrous runs, with the vessel initially filled with
242 20 ml water. After lowering the pressure vessel onto the sand bath, the vessel was
243 connected to the high liquid water pressure line and allowed to attain its maximum
244 vapour pressure of 175 bar (in about 30 minutes), before the addition of more water to
245 increase the pressure. This procedure is employed to prevent too much water being
246 added to the vessel which might lead to the generation of over pressure in excess of the
247 pressure limit of the system. To apply high liquid water pressure to the system (with the
248 aid of a compressed air driven liquid pump), the emergency pressure release valve B
249 was first closed, and valve A opened until a pressure slightly higher than the vapour
250 pressure of the experiment is displayed on the external pressure gauge. This was

undertaken to avoid losing any content of the vessel when the reactor valve C is opened. High liquid water pressure was then applied to the system by first opening valve C and immediately gradually opening valve A to add more distilled water into the reaction vessel. When the required pressure was attained, valve C was closed to isolate the reactor from the high water pressure line, and valve A was also closed to prevent more water going to the pressure line. Valve B was opened to vent the excess pressure on the line. The experiment was then allowed to run (leaving valve C tightly closed to avoid losing generated products) for the required time, after which the sand bath is switched off and left to cool to ambient temperature before product recovery.

The total internal volume of the empty pressure vessel and its associated pipe work and pressure gauge was estimated to be about 31 ml by pressurising with nitrogen gas from a nitrogen cylinder set to 2 bar, and measuring the volume of gas released. It is important to note that overpressure was not generated during the low pressure (175 bar) or 500 bar and 900 bar experiments due to the small amount of gas generated, and the recorded final pressure after 24 h being the same as pressure at the start of the experiment.

In order to test if any gas in the system was lost in the process of pressurising the vessel, a control experiment was conducted at 350 °C for 50 minutes at a pressure of 500 bar using the same oil sample being studied. The short time used for the control experiment was to ensure the oil did not thermally crack. The volume of gas collected after the control experiment was found to be equal to the volume of nitrogen pumped into the system at 2 bar before the experiment started. This indicated that gas has not been lost either during pressurisation, pressure build up in the vessel or during gas

sampling from the reactor after the experiments. A flow chart showing the pyrolysis conditions, products recovery and analysis are shown in Figure 2, and the four separate experiments carried out on both the oil and *n*-hexadecane as listed below:

i. 20 bar (low pressure non-hydrous pyrolysis)

ii. 175 bar (15 ml water, normal low pressure hydrous pyrolysis)

iii. 500 bar (high liquid water pressure pyrolysis)

iv. 900 bar (high liquid water pressure pyrolysis)

No attempt has been made to separate the effects of water and inert pressure at low pressures since the emphasis here is understanding the impact high water pressures on the initial stages of cracking.

2.2. Gas analysis

To recover the generated gas, the high water pressure line was disconnected and a connector attached to valve C. The generated gas was collected at ambient temperature (via the connector by opening valve C) with the aid of a gas tight syringe and transferred to a gas bag (after the total volume had been recorded) and immediately analysed. The gas generated from the *n*-hexadecane experiments were analysed on a Carlo Erba HRGC 5300 GC fitted with a FID detector operating at 200 °C. 10 µl of gas samples were injected at 100 °C with separation performed on a Varian Poraplot-Q fused silica 25 m x 0.32 mm x 10 µm column, with helium as the carrier gas. The oven temperature was programmed from 70 °C (2 min hold) to 90 °C (3 min hold) at 40 °C min^{-1}, then to 140 °C (3 min hold) at 40 °C min^{-1}, and finally to 180 °C (49 min hold) at

40 °C min^{-1}. The gas from the oil cracking experiments were analysed on a Clarus 580 GC fitted with a FID and TCD detectors operating at 200 °C. 100 µl of gas samples were injected (split ratio 10:1) at 250 °C with separation performed on an alumina plot fused silica 30 m x 0.32 mm x 10 µm column, with helium as the carrier gas. The oven temperature was programmed from 60 °C (13 min hold) to 180 °C (10 min hold) at 10 °C min^{-1}. Individual gas yields were determined quantitatively in relation to methane (injected separately) as an external gas standard. The total yield of the hydrocarbon gases generated was calculated using the total volume of generated gas collected in relation to the aliquot volume of gas introduced to the GC, using relative response factors of individual C_2-C_5 gases to methane predetermined from a standard mixture of C_1-C_5 gases. The C_5 gases were not reported for *n*-hexadecane because only C_1-C_3 and butane gases were correctly identified because of the age of the instrument and the old software used for the GC.

2.3. GC and GC-MS analysis of GOM bitumen, oils and *n*-hexadecane

After gas analysis, aliquots of oil and *n*-hexadecane were collected for GC and GC-MS analysis respectively, and the asphaltene content of the oil left was determined based on the weight of oil remaining as previously described elsewhere (Russell et al., 2004). The GC analysis of the initial, cracked whole oil and GOM bitumen fractions were carried out using an Agilent 6890 GC fitted with FID at 350 °C. Injections were performed in split mode (split ratio 100:1), with separation achieved on a DB-1 fused silica capillary column (100 m). Helium was employed as the carrier gas, with a temperature programme of -20 °C cryogenic (hold for 0 min) to 320 °C (hold for 30 min) at 10 °C min^{-1}. GC-MS analysis of the cracked *n*-hexadecane products were

318 performed on a Varian CP-3800 GC interfaced to a Varian 1200 MS (ionising energy
319 70 eV, source temperature 280 °C). Injections were performed in split mode (split ratio
320 30:1) and eluted components monitored in full scan mode (*m/z* 50-450), turning off the
321 instrument at the elution time of *n*-hexadecane to avoid damaging the filament.
322 Separation was achieved on a VF-1MS fused silica capillary column (50 m x 0.25 mm
323 internal diameter, 0.25 m thickness), with helium as the carrier gas, and an oven
324 programme of 50 °C (hold for 2 min) to 300 °C (hold for 20.5 min) at 4 °C min^{-1}.

325 **2.4. Hydropyrolysis of GOM bitumen asphaltene and GC-MS analysis**

326 The asphaltene fraction isolated from the GOM bitumen was subjected to
327 hydropyrolysis as described in detail elsewhere (Murray et al., 1998; Russell et al.,
328 2004). Briefly, the sample (50 mg) was pyrolysed on a bed of sulphided molybdenum
329 catalyst (250 mg), with resistive heating from 50 °C to 250 °C at 300 °C min^{-1}, and then
330 250 °C to 520 °C (hold for 2 min) at 8 °C min^{-1}, under a hydrogen pressure of 15 MPa.
331 A hydrogen sweep gas flow of 5 l min^{-1}, (measured at ambient temperature and
332 pressure), ensured that the products were quickly removed from the reactor vessel, with
333 the products trapped on dry ice cooled silica. The aliphatic, aromatic and polar fractions
334 of the hydropyrolysates were separated by silica gel / alumina adsorption
335 chromatography with successive elutions of *n*-hexane, *n*-hexane/DCM (3:2 v/v) and
336 DCM/methanol (1:1 v/v), with the aliphatic fraction then analysed using the same GC-
337 MS as used for *n*-hexadecane above using an oven programme of 50 °C (hold for 2 min)
338 to 300 °C (hold for 33 min) at 5 °C min^{-1}. Analysis were performed in full scan mode
339 (*m/z* 50-450) and selected ions monitoring *m/z* 191 (hopanes) and *m/z* 217 (steranes)
340 separately.

3. Results and discussion

3.1 Gas yields

Table 1 presents the individual and total (C_1-C_5) gas yields (mg/g of carbon of pyrolysed oil and *n*-hexadecane). The gas yields are low as expected for the initial stages of cracking for both the oil and *n*-hexadecane. However, they are highest under non-hydrous low pressure (20 bar) conditions and reduce in going to normal hydrous pressure (175 bar), with the C_1-C_5 yield 44% lower compared to the non-hydrous (20 bar) yield for the oil. This confirms that a combination of increasing pressure and water retards oil cracking to gas, consistent with previous studies (Brooks et al., 1971; Hesp and Rigby 1973). The gas yields continue to fall with increasing water pressure, with the alkene formation strongly suppressed. At 500 bar, the C_1-C_5 hydrocarbon gas yields decrease slightly compared to 175 bar, while at 900 bar the gas yield is 36% and 23% lower in relation to the 175 bar and 500 bar yields, respectively. The trends in gas yields for both the initial stages of cracking for oil and *n*-hexadecane pyrolysis are consistent to those observed for our previous studies for the pyrolysis of coals between 500 and 900 bar water pressure at 350 °C (Uguna et al., 2012a) and for Kimmeridge Clay Type II source rock pyrolysed between 310 and 350 °C at 500 bar water pressure (Carr et al., 2009; Uguna et al., 2012b; 2013). However, when the gas yields obtained here at 500 and 900 bar are compared to our previous studies on coals and Kimmeridge Clay type II source rock (Carr et al., 2009: Uguna et al., 2012a; 2012b; 2016) the sequence of the retardation effect of pressure is *n*-hexadecane (most retarded) > oil > perhydrous coals > Type II source rocks (least retarded). The C_1-C_5 gas yield for oil pyrolysis at 900 bar in this study is 6.5 times lower compared to Kimmeridge clay also

364 pyrolysed at 900 bar under the same temperature and time (Uguna et al., 2016). This
365 suggests that the retardation effect of pressure is greater for the initial stages of oil
366 cracking than for source rock maturation.

367 The reduction in gas yield in the presence of water (175 bar hydrous conditions)
368 compared to the absence of water (non-hydrous conditions) observed here is the
369 opposite observed previously for source rocks and kerogens. It has been widely
370 reported that gas and liquid hydrocarbon yields from kerogens, petroleum source rocks
371 and coals are significantly higher under hydrous compared to non-hydrous conditions
372 (Comet et al., 1986; Andresen et al., 1993; Kuangzong et al., 1994; Michels and
373 Landais 1994; Lewan 1997; Behar et al., 2003). The higher products yield under
374 hydrous conditions reported in the above studies is due to water playing the role of a
375 reactive medium by transferring hydrogen and oxygen to kerogen termed the chemical
376 effect of water. Our previous study (Carr et al., 2009) investigated the chemical effect
377 of water on hydrocarbon gas generation by comparing non-hydrous pyrolysis to hydrous
378 pyrolysis using different volumes of water for Kimmeridge Clay pyrolysed at 350 °C
379 for 24 h. This study showed that hydrocarbon (C_1-C_4) gas yields was higher (24 mg/g
380 TOC) with 10 ml water (155 bar) in the vessel compared to non-hydrous (15 bar) yield
381 (16 mg/g TOC), and when the water volume was doubled to 20 ml (180 bar) the gas
382 yield reduced to 11 mg/g TOC. Also in our previous study comparing gas and bitumen
383 yields under hydrous (20 ml water, 175 bar pressure) and non-hydrous conditions
384 showed that hydrocarbon (C_1-C_4) gas yields was lower and bitumen yield higher under
385 hydrous compared to non-hydrous conditions for coals pyrolysed at 350°C for 24 h
386 (Uguna et al., 2012a).

These studies show that water has a chemical effect in promoting kerogen conversion to liquid and gaseous hydrocarbon under hydrous conditions. However, the reduction in gas yield in the presence of water under normal hydrous conditions (175 bar) observed in this study confirms that water is an inhibitor in both oil and *n*-hexadecane cracking reactions as opposed to a reactive medium in kerogen conversion reactions (Comet et al., 1986; Andresen et al., 1993; Kuangzong et al., 1994; Michels and Landais 1994; Lewan 1997; Behar et al., 2003; Carr et al., 2009). The retardation of oil and *n*-hexadecane cracking with increasing pressure reflects the increase in the Ea (activation energy) of the reactions with increasing pressure.

3.2 Cracked oils and *n*-hexadecane

The whole oil GC traces are presented in Figures 3a and 3b. Under non-hydrous and 175 bar conditions, no discernible changes were observed in the *n*-alkane distribution in the whole oil GC since the overall extent of cracking is low at a temperature of 350 °C for a period of 24 h, consistent with the low extent of cracking. The 500 and 900 bar GC traces visually show higher abundance of heavier *n*-alkanes ($>C_{20}$) compared to the initial, non-hydrous (20 bar) and 175 bar oils. The 500 and 900 bar oils GC traces also shows unresolved complex mixture (UCM). This was very evident in the 900 bar oil when compared to the 175 bar oil (Figure 3b). The GC-MS total ion chromatograms for *n*-hexadecane cracking are presented in Figures 4a and 4b. The non-hydrous (20 bar) trace show a complex mixture of straight and branched chain alkanes in the C_{18}-C_{31} region. Under 175 bar hydrous conditions, the C_{18}-C_{31} alkanes mixture were completely absent, but increase in water pressure to 500 and 900 bar resulted to their formation with their abundance visually more at 900 bar.

410 The higher abundance of higher molecular weight *n*-alkanes (>C_{20}) observed for
411 the 500 and 900 bar oils (Figures 3a and 3b) indicate that water pressure conditions
412 gave rise to higher boiling, higher gravity viscous oils, the trend being most pronounced
413 for the 900 bar oil (Figures 3a and 3b). The unresolved complex mixture (UCM) was
414 also very evident in the 900 bar oil when compared to 175 bar oil (Figure 3b), and arises
415 from combination reactions involving the higher boiling materials (>C_6). These
416 combination reactions are exothermic unlike cracking reactions which are endothermic,
417 and exothermic reactions are more favoured under high pressures than cracking
418 reactions, as shown by the retardation of coal to gas conversion reactions at 350 °C
419 under pressures of 500 and 900 bar (Uguna et al., 2012a). To show that the 500 and 900
420 bar oils are heavier (contain higher abundance of *n*-alkanes >C_{20}) than the initial, non-
421 hydrous and 175 bar oil, some peak area ratios from the whole oil GC trace and the
422 asphaltene contents of the oils were used below. The use of peak area ratios of *n*-
423 alkanes to determine their abundance in the oils was preferred to the use of an internal
424 standard to quantify their concentrations. This was to avoid introducing organic solvent
425 to the oils which will have resulted in the light ends (gasoline range hydrocarbons)
426 being lost due to co-elution with the solvent front. The peak area ratios used are;
427 toluene/*n*C_7, toluene/*n*C_{28}, methylcyclohexane/*n*C_7, short to long chain *n*-alkanes
428 [(*n*C_6+*n*C_7+*n*C_8)/(*n*C_{27}+*n*C_{28}+*n*C_{29}) and (*n*C_6+*n*C_7+*n*C_8)/(*n*C_{30}+*n*C_{31}+*n*C_{32})], initial
429 oil/pyrolysed oil short chain (*n*C_6+*n*C_7+*n*C_8+*n*C_9) *n*-alkanes, and initial oil/pyrolysed oil
430 long chain (*n*C_{27}+*n*C_{28}+*n*C_{29}+*n*C_{30}) and (*n*C_{31}+*n*C_{32}+*n*C_{33}+*n*C_{34}) *n*-alkanes.

431 Considering the peak area ratios of toluene to C_{28} *n*-alkane and short to long
432 chain *n*-alkanes for the initial and pyrolysed oils (Figure 5), these ratios initially
433 increase from the initial oil to a maximum at 175 bar before decreasing with an increase

434 in pressure to values lower than the initial oil. The increase shown going from the
435 initial to non-hydrous and 175 bar shows that the non-hydrous and 175 bar oil contains
436 lower abundance of C_{27}-C_{32} *n*-alkanes than the initial oil which resulted from their
437 cracking to form more C_6-C_8 *n*-alkanes. However, the lower values shown at 500 and
438 900 bar compared to the initial oil indicates that the 500 and 900 bar oils contain higher
439 abundance of C_{27}-C_{32} *n*-alkanes than the initial oil, which should not be the case if
440 cracking is occurring. This again occurs due to the preferential combination of smaller
441 hydrocarbon molecules into more complex higher boiling point hydrocarbons. The
442 toluene to *n*-heptane and methylcyclohexane to *n*-heptane peak area ratios (Figure 5)
443 show that the relative amounts of these compounds are the same for both the initial and
444 pyrolysed oils, suggesting that their relative stabilities are similar under the
445 experimental conditions used.

446 When the ratio of the initial to pyrolysed oil short chain *n*-alkanes (Figure 6) is
447 considered, the values change from 0.89 and 0.93 under non-hydrous (20 bar) and 175
448 bar conditions respectively to 1.24 at 500 bar and 1.48 at 900 bar. The ratio of <1
449 obtained under non-hydrous and 175 bar shows that the oils contains more C_6-C_9 *n*-
450 alkanes than the initial oil due to some cracking of high molecular weight hydrocarbons.
451 However, the change in the ratio from being <1 under 175 bar hydrous conditions in
452 which very small cracking occurred to >1 at 500 and 900 bar suggests that the cracking
453 to smaller hydrocarbons is being increasingly restricted, and the 500 and 900 bar oils
454 contain lesser amounts of C_6-C_9 *n*-alkanes than the initial oil. This is again due to
455 combination reactions involving lower molecular hydrocarbons into larger and more
456 complex hydrocarbons.

457 Figure 6 also presents the initial to pyrolysed oils long chain *n*-alkanes, the
458 initial to pyrolysed oil (nC_{31}-C_{34}) ratio initially increased going from 1.24 at 20 bar
459 (non-hydrous) to 1.59 at 175 bar before reducing significantly with increase in water
460 pressure to 0.79 and 0.67 at 500 and 900 bar respectively. The initial to pyrolysed oils
461 (nC_{27}-nC_{30}) ratios were 1.08 (non-hydrous) and 1.12 (175 bar), but were 0.73 and 0.66
462 in the 500 and 900 bar oils. The higher ratios (>1) obtained for the initial to non-
463 hydrous and 175 bar oil again indicate that the abundance of C_{27}-C_{34} *n*-alkanes are
464 lower in the non-hydrous and 175 bar pyrolysed oils than in the initial oil, which shows
465 that the higher molecular weight (C_{27}-C_{34}) alkanes were being cracked to lighter
466 hydrocarbons ($<C_{10}$) and gas. The reduction in both ratios (<1) going to 500 and 900
467 bar indicate that the abundance of C_{27}-C_{34} *n*-alkanes in the 500 and 900 bar oils is
468 higher than in the initial oil which should not be the case if cracking is occurring. The
469 change in the values between 20 bar (non-hydrous) and 175 bar for both the (nC_{27}-nC_{30})
470 and (nC_{31}-nC_{34}) ratios between the initial oil and the pyrolysed oils shows that the
471 largest increase occur in the longer chain *n*-alkanes, suggesting that these were cracked
472 more easily under low pressure conditions than the nC_{27}-nC_{30} alkanes. Interestingly, the
473 values for both the (nC_{27}-nC_{30}) and (nC_{31}-nC_{34}) ratios between the initial oil and the
474 pyrolysed oils are very similar at 500 and 900 bar at 350 °C.

475 The increase in abundance of C_{27}-C_{34} *n*-alkanes together with the reduction in
476 C_6-C_9 *n*-alkane abundance in the oils with increase in water pressure provide more
477 evidence that the higher amounts of long chain hydrocarbons in the 500 and 900 bar oils
478 results from combination reactions involving lower molecular weight hydrocarbons.
479 The fact that the amount of C_6-C_9 *n*-alkanes is lowest and the C_{27}-C_{34} *n*-alkanes is
480 highest in the 900 bar oil, indicate that combination reactions are more favoured over

481 cracking reactions at 900 bar and 350 °C, meaning cracking reactions were being
482 replaced by combination reactions at high pressures. The asphaltene content of the
483 cracked oils also increased significantly from 0.4% (initial oil) to 1.1% and 1.3% for the
484 non-hydrous and 175 bar oils respectively due to cracking. The 900 bar oil asphaltene
485 increased further to 1.9% despite the extent of cracking decreasing with increase in
486 pressure. Like the combination reactions observed involving lower molecular weight
487 hydrocarbons, asphaltene formation is a volume reduction process and should be
488 favoured also at high pressures.

489 For *n*-hexadecane, the product distribution from the non-hydrous (20 bar)
490 pyrolysis (Figures 4a and 4b) was entirely consistent with previous studies using similar
491 conditions (Ford, 1986; Wu et al., 1996), with the lower molecular weight ($<C_{14}$)
492 hydrocarbons being mainly straight chain alkenes and alkanes, and the higher molecular
493 weight ($>C_{18}$) hydrocarbons containing branched and straight chain alkanes in the C_{18}-
494 C_{31} region. Ford (1986) and Wu et al. (1996) concluded that the C_{18}-C_{31} straight and
495 branched chain alkanes were formed by alkylation reactions between lower molecular
496 weight ($<C_{14}$) alkenes and C_{16} radicals. Under normal pressure (175 bar) hydrous
497 conditions (Figures 4a and 4b), the concentration of $<C_{14}$ alkenes decreased and the
498 formation of C_{18}-C_{31} alkanes was completely suppressed. The reduction in $<C_{14}$ alkenes
499 concentration at 175 bar is due to hydrogenation of alkenes to alkanes, as well as
500 suppression of alkene generation reactions under normal hydrous conditions. The
501 absence of C_{18}-C_{31} alkanes in the 175 bar product is due to insufficient $<C_{14}$ alkenes (as
502 they were hydrogenated to alkanes) that can react with C_{16} radicals to form C_{18}-C_{31}
503 alkanes. The 500 and 900 bar water pressure products lacked $<C_{14}$ alkenes but contain
504 C_{18}-C_{31} straight and branched chain alkanes (Figures 4a and 4b), with the concentration

505 increasing further to 900 bar. In a study on the effects of pressure on the cracking of *n*-
506 tetradecane (*n*-C_{14}) at temperatures between 250 and 450 °C and at pressures between
507 0.001 and 1000 bar in gold-bag pyrolysis experiments, Michels et al. (2015) observed
508 maxima in the bell-shaped *n*-alkane conversion curve. The pressure at which the
509 maxima occurred increased with increasing temperature. The proportion of
510 monomolecular vs bimolecular reactions controls the extent of conversion (bell shape
511 curves) under the conditions used, i.e. confined, non-hydrous pyrolysis. For each
512 temperature the curve profile changed. Many contradictions into the effects of pressure
513 on hydrocarbon pyrolysis published ("retardation vs acceleration" of reaction) arise
514 from the lack of understanding of this complex behaviour. While this issue is
515 undoubtedly correct, the effect that water has on the reactions as highlighted by the
516 studies of Brooks et al. (1971), Hesp and Rigby (1973), and Hoering (1984) was
517 ignored by Michels and co-workers (e,g. Michels et al., 2015; Panifolva et al., 2015),
518 who claimed that non hydrous experimental conditions can replicate the cracking of oil
519 in deeply buried reservoirs. Comparing the results at 900 bar with those obtained at
520 either 175 bar (hydrous) or 500 bar water pressure for both Oseberg oil and *n*-
521 hexadecane here shows that at high water pressure the gas yield is reduced, the presence
522 of alkenes is virtually eliminated, and the high molecular weight products are increased.
523 The high-pressure results are inconsistent with the more efficient cracking observed by
524 Michels et al. (1995) for the results obtained from hydrous as opposed to confined
525 (gold-bag) pyrolysis. As already discussed, this effect is due to the conservation of
526 energy law, and the absence of sufficient thermal energy (even at 350 °C) to provide the
527 energy for both bond rupture to create the radicals required for the generation of low
528 molecular weight compounds, i.e. gases, and pV work required for the product

529 formation. Lannuzel et al. (2010) observed the absence of alkenes in high pressure (700
530 bar) gold-bag pyrolysis at 350 °C, and the absence of alkenes in the high-water pressure
531 results in this study appears to be consistent with this.

532 The fact that the formation of the C_{18}-C_{31} normal and branched alkanes were
533 hindered at 175 bar indicates that their formation at 500 and 900 bar water pressure is
534 due to combination reactions induced by water pressure, and we believe the reaction
535 involves $<C_{14}$ alkenes and C_{16} radicals since $<C_{14}$ alkenes were absent under the high
536 water pressure conditions. The absence of $<C_{14}$ alkenes under 500 and 900 bar is due to
537 a combination of their suppression, and combination reactions. Combination reaction
538 occurred under 500 and 900 bar pressures conditions because the vessel is
539 predominantly full of water and there was no vapour present where the alkenes can be
540 hydrogenated to alkanes as was the case at 175 bar. The hydrogenation of alkenes to
541 alkanes and suppression of alkene formation observed in this study under high water
542 pressure conditions explains why alkenes are not present in natural oils, and provide
543 evidence that high water pressure pyrolysis closely simulates natural conditions present
544 in geological basins.

545 **3.3 Evidence for bitumen formation by combination reactions**

546 The GOM bitumen is not biodegraded containing light *n*-alkanes, contains 52%
547 asphaltene, and the GC chromatogram (Figure 7a) resembles those of the 500 and 900
548 bar pyrolysed oils (Figures 3a and 3b), in showing an unresolved complex mixture
549 (UCM), below the chromatogram baseline in the region of the extended ($>nC_{20}$) *n*-
550 alkanes. The asphaltene content of the bitumen is significantly higher than the 900 bar
551 oil, and the unresolved complex mixture more pronounced. Solli and Leplat (1986),

552 Jones et al. (1988), and Sofer (1988) all reported that alkanes were generated by
553 asphaltene hydrous pyrolysis by cracking, which is in contrast to the asphaltene
554 formation by high pressure pyrolysis observed in this study. We believe that
555 combination reactions which increased the asphaltene content and higher molecular
556 weight *n*-alkanes of the 500 and 900 bar oils and the formation of C_{18}-C_{31} straight and
557 branched alkanes for *n*-hexadecane pyrolysis at 500 and 900 bar is also responsible for
558 the high asphaltene content of the GOM bitumen. To investigate this, the maturities of
559 the free biomarkers were compared to the asphaltene bound biomarkers released by
560 catalytic hydropyrolysis (Murray et al., 1998; Russell et al., 2004). The C_{29} ααα S /
561 (ααα S + ααα R) and C_{29} αββ / ((ααα S + ααα R) + αββ) free sterane (Figure 7b)
562 ratios were 0.52 and 0.49 respectively. This was similar to the ratios of 0.53 (C_{29} ααα S
563 / ααα S + ααα R) and 0.52 [C_{29} αββ / (ααα S + ααα R) + αββ] obtained for the
564 asphaltene bound steranes (Figure 7c). The C_{31} and C_{32} ααα S / (ααα S+ ααα R) free
565 hopane ratios were 0.60 and 0.58 respectively, also similar to the asphaltene bound
566 hopane ratios 0.60 (C_{31} ααα S / (ααα S+ ααα R)) and 0.59 (C_{32} ααα S / (ααα S+ ααα
567 R)). Asphaltene bound biomarkers have been found to be generally less mature than
568 free biomarkers (Murray et al., 1998; Russell et al., 2004). The fact that the free and
569 asphaltene bound biomarkers for the GOM bitumen are of similar maturity further
570 suggest that the bitumen may have been formed from oil by combination reaction
571 induced by pressure and the free phase biomarkers may have been incorporated into the
572 asphaltene during this process.

573 **3.4 General discussion**

574 The magnitude of the retardation effects of pressure on the initial stages of oil
575 cracking is much greater than found in previous studies using confined gold bags
576 pyrolysis method (Hill et al., 1996; Al Darouich et al., 2006) that generally show less
577 retardation effect compared to the unconfined water pyrolysis method used here. The
578 decomposition of oil to gas occurs via beta scission of hydrocarbons to generate free
579 radicals. Two types of radicals play a part in the pyrolysis mechanism of saturated
580 hydrocarbons (Bounaceur et al., 2002a): radicals that decompose by monomolecular
581 reactions and radicals that react by bimolecular reactions. Clearly, the former involve
582 volume expansion and intuitively will be considerably more retarded by pressure. The
583 results also need to be considered with respect to transition state theory where pressure
584 is likely to increase the pV work term in the activation energy, Ea. In the case of oil
585 cracking in reservoirs in geological basins, the pore spaces not filled with oil are
586 initially filled with water prior to oil cracking, and as noted above the incompressible
587 nature of the water can be viewed as increasing the pV work term required as the forces
588 opposing the formation of the activated complex increase.

589 The ability of high water pressure to promote combination reactions resulting in
590 more viscous oil have been observed for the first time under laboratory water pressure
591 conditions. This explains why oils can be stable, becoming heavier and potentially even
592 forming bitumens like the GOM bitumen shown here, under the high water pressure
593 regimes found in geological basins. Indeed, for Caillou Island (Louisiana) oils, Price
594 (1990) reported an increase in API from 30° at 9000 ft. to 50° at 19000 ft., before
595 reducing rapidly to 35° API at 20000 ft., a trend that might be expected if increasing
596 water pressure was producing heavy oil. Combination reactions are exothermic, which
597 means that they would be favoured in cooler high pressure basins, e.g. the Gulf of

598 Mexico, and lower API gravity oils with higher asphaltene content than used in this
599 study will more likely favour this process. Moreover, much of the bitumen previously
600 described as the pyrobitumenic residue after oil cracking has possibly been incorrectly
601 identified. Indeed characterisation of the supposed 'pyrobitumens' in the high
602 temperature (190 °C) high pressure North Sea Upper Jurassic Fulmar Formation
603 (Scotchman et al., 2006) have shown that the 'pyrobitumens' are degraded residues of
604 normal oil window mature North Sea oils, e.g., deasphaltation (Wilhelms and Larter,
605 1995), and have not formed by oil cracking as proposed by Vandenbroucke et al.
606 (1999). In this case may be the high temperatures are preventing the exothermic
607 combination reactions, whereas the high pressures are preventing the endothermic
608 cracking reactions. Much more work is required into this area of research to fully
609 understand heavy oil formation in geological basins.

610 To attempt extrapolation from 350 °C to the temperatures in geological basins,
611 the chemical effects of water in promoting conversion will possibly be lowered due to
612 lower water solubility of hydrocarbons. However, the physical effect of pressurised
613 water will probably be emphasised even more because the viscosity of oil will increase
614 significantly. Also in conjunction with pressure, it is recognised that other variables,
615 such as pH, Eh, mineralogy and porosity could all have a significant role to play.
616 Further, Michels et al. (1995) concluded that as well as the chemical composition of the
617 diagenetic fluids (aqueous solutions and gases), their physical relationship with bitumen
618 and oils, and the interactions between water and the organic compounds within the
619 organic phases, as well as temperature and pressure parameters need to be considered
620 when extrapolating the chemical mechanisms observed in laboratory to the natural
621 environment. However, whilst all these factors must be considered, the reduced

622 cracking observed in conjunction with the combination reactions favoured by high
623 water pressure provides a new means for rationalising the observed thermal stability of
624 oils and heavy oil formation in high pressure basins.

625 **4. Conclusions and implications**

626 1. The cracking of oil and *n*-hexadecane to hydrocarbon gases was retarded in the
627 presence of water under 175 bar low pressure hydrous conditions compared to non-
628 hydrous (absence of water). The retardation effect of pressure was more significant at
629 500 and 900 bar water pressure compared to 175 bar with the alkene gases most
630 retarded.

631 2. The cracking of oil and *n*-hexadecane to lower molecular weight (C_6-C_9)
632 hydrocarbons was retarded under 500 and 900 bar water pressure compared to 175 bar,
633 with the effect being most significant at 900 bar.

634 3. At 500 and 900 bar water pressure combination reactions occurred, replacing
635 cracking reactions. These increased the abundance of heavier *n*-alkanes ($>C_{20}$) present
636 in both oil and *n*-hexadecane, the amount of unresolved complex material (UCM) and
637 asphaltene content of the oil.

638 4. Combination reactions observed at high water pressure for the first time in this study
639 provide a new mechanism for rationalising the thermal stability of oils, and producing
640 heavy oils at temperatures above those at which biodegradation can occur.

641 5. This study have demonstrated from the maturity of the bound biomarkers released by
642 hydropyrolysis that bitumen from the high pressure Gulf of Mexico basin have been
643 formed from lighter oil components via combination reactions.

644 The implications from this study are that in deep petroleum basins and reservoirs
645 with high pressures, the retardation effect of pressure on oil cracking will be far more
646 significant than is currently thought. Oil will be far more thermally stable, and
647 combination reactions resulting in more viscous oil will be far more likely to occur than
648 observed in this study. This is due to temperature been lower and pressures (regardless
649 of whether overpressure is present) higher in geological basins than temperature of 350
650 °C and maximum pressure of 900 bar used in this study.

651 **Acknowledgments**

652 The authors would like to thank Statoil and Woodside Energy Ltd., for financial
653 support. The views published in this paper reflect those of the authors and are not
654 indicative of the views or company policy of either Statoil or Woodside Energy. The
655 authors would also like to thank the two anonymous reviewers for their effort in
656 reviewing this paper, and the associate editor Geoffrey Abbott for his corrections and
657 suggestion which have improved it.

658

659
660

661

662

663

664

References

Abbott, G.D., Bennett, B., Petch, G.S., 1995. The thermal degradation of 5α(H) – cholestane during closed-system pyrolysis. Geochimica et Cosmochimica Acta 59, 2259-2264.

Al Darouich, T., Behar, F., Largeau, C., 2006. Pressure effect on the thermal cracking of the light aromatic fraction of Safaniya crude oil – Implications for deep prospects. Organic Geochemistry 37, 1155–1169.

Andresen, B., Barth, T., Irwin, H., 1993. Yields and carbon isotopic composition of pyrolysis products from artificial maturation processes. Chemical Geology 106, 103-119.

Bailey, N.J.L., Evans, C.R., Milner, C.W.D., 1974. Applying Petroleum Geochemistry to Search for Oil: Examples from Western Canada Basin. American Association of Petroleum Geology Bulletin 58, 2284–2294.

Barker, C., 1990. Calculated volume and pressure changes during the thermal cracking of oil to gas in reservoirs. AAPG Bulletin 74, 1254–1261.

Behar, F., Kressmann, S., Rudkiewicz, J.L., Vandenbroucke, M., 1992. Experimental simulation in a confined system and kinetic modelling of kerogen and oil cracking. Organic Geochemistry 19, 173–189.

Behar, F., Vandenbroucke M., 1996. Experimental determination of rate constants of the *n*-C_{25} thermal cracking at 120, 140, and 800 bar: Implication for the high pressure/high temperature prospects. Energy & Fuels 10, 932–940.

686 Behar, F., Tang, Y., Liu, J., 1997a. Comparison of rate constants for some molecular
687 tracers generated during artificial maturation of kerogens: influence of kerogen
688 type. Organic Geochemistry 26, 281–287.

689 Behar, F., Vandenbroucke, M., Tang, Y., Marquis, F., Espitalié, J., 1997b. Thermal
690 cracking of kerogen in open and closed systems: determination of kinetic
691 parameters and stoichiometric coefficients for oil and gas generation. Organic
692 Geochemistry 26, 321–339.

693 Behar, F., Budzinski, H., Vandenbroucke, M., Tang, Y., 1999. Methane generation from
694 oil cracking: kinetics of 9-methylphenanthrene cracking and comparison with
695 other pure compounds and oil fractions. Energy & Fuels 13, 471–481.

696 Behar, F., Lorant, F., Budzinski, H., Desavis, E., 2002. Thermal stability of
697 alkylaromatics in natural systems: kinetics of thermal decomposition of
698 dodecylbenzene. Energy & Fuels 16, 831–841.

699 Behar, F., Lewan, M. D., Lorant, F., Vandenbroucke, M., 2003. Comparison of artificial
700 maturation of lignite in hydrous and nonhydrous conditions. Organic
701 Geochemistry 34, 575-600.

702 Behar, F., Lorant., F., Mazeas, L., 2008. Elaboration of a new compositional kinetic
703 schema for oil cracking. Organic Geochemistry 39, 764–782.

704 Bounaceur, R., Scacchi, G., Marquaire, P.M., Dominé, F., 2000. Mechanistic modelling
705 of the thermal cracking of tetralin. Industrial Engineering and Chemical
706 Research 39, 4152–4165.

707 Bounaceur, R., Warth, V., Marquaire, P.M., Scacchi, G., Dominé, F., Dessort, D.,
708 Pradier, B., Brévart, O., 2002a. Modelling of hydrocarbons pyrolysis at low
709 temperature. Automatic generation of free radicals mechanisms. Journal of
710 Analytical and Applied Pyrolysis 64, 103–122.

711 Bounaceur, R.; Scacchi, G.; Marquaire, P.-M.; Domine´, F.; Brevart, O.; Dessort, D.;
712 Pradier, B. 2002b. Inhibiting effect of tetralin on the pyrolytic decomposition of
713 hexadecane. Comparison with toluene. Industrial Engineering and Chemical
714 Research 41, 4689–4701.

715 Brooks, J.D., Hesp, W.R., Rigby, D., 1971. The natural conversion of oil to gas in
716 sediments in the Cooper basin: APEA Journal 11, 121–125.

717 Burnham, A.K., Gregg, H.R., Ward, R.L., Knauss, K.G., Copenhaver, S.A., Reynolds,
718 J.G., Sanborn, R., 1997. Decomposition kinetics and mechanism of *n*-
719 hexadecane-1,2-$^{13}C_2$ and dodec-1-ene-1,2-$^{13}C_2$ doped in petroleum and *n*-
720 hexadecane. Geochimica et Cosmochimica Acta, 61, 3725–3737.

721 Burnham, A.K., Sanborn, R.H., Gregg, H.R., 1998. Thermal dealkylation of
722 dodecylbenzene and dodecylcyclohexane. Organic Geochemistry 28, 755–758.

723 Burklé-Vitzthum, V., Michels, R., Scacchi, G., Marquaire, P-M., 2003. Mechanistic
724 modelling of the thermal cracking of decylbenzene. Application to the prediction
725 of its thermal stability at geological conditions. Industrial Engineering and
726 Chemical Research 42, 5791–5808.

727 Burklé-Vitzthum, V., Michels, R., Scacchi, G., Marquaire, P-M., Dessort, D., Pradier,
728 B., Brevart, O., 2004. Kinetic effect of alkylaromatics on the thermal stability of
729 hydrocarbons under geological conditions. Organic Geochemistry 35, 3–31.

730 Burklé-Vitzthum, V., Michels, R., 2005. Experimental study and modelling of the role
731 of hydronaphthalenics on the thermal stability of hydrocarbons under laboratory
732 and geological conditions. Industrial Engineering and Chemical Research 44,
733 8972–8987.

734 Carr, A.D., Snape, C.E., Meredith, W., Uguna, C., Scotchman, I.C., Davis, R.C., 2009.
735 The effect of water pressure on hydrocarbon generation reactions: some
736 inferences from laboratory experiments. Petroleum Geoscience 15, 17–26.

737 Comet, P. A., McEvoy, J., Giger, W., Douglas, A. G., 1986. Hydrous and anhydrous
738 pyrolysis of DSDP Leg 75 kerogens-A comparative study using a biological
739 marker approach. Organic Geochemistry 9, 171-182.

740 Connan, J., Le Tran, K., van der Weide, B.M., 1975. Alteration of petroleum in
741 reservoirs. Proceedings of the 9th World Petroleum Congress, Tokyo, vol. 2,
742 171–178.

743 Dahl, B., Speers, G.C., 1985. Organic Geochemistry of the Oseberg Field (1). In:
744 Graham & Trotman (Eds.), Petroleum geochemistry in exploration of the
745 Norwegian shelf. Norwegian petroleum society, 185–196.

746 Dartiguelongue, C., Behar, F., Budzinski, H., Scacchi, G., Marquaire, P.M., 2006.
747 Thermal stability of dibenzothiophene in closed system pyrolysis: experimental
748 study and kinetic modelling. Organic Geochemistry 37, 98–116.

749 Dieckmann, V., Schenk, H.J., Horsfield, B., Welte, D.H., 1998. Kinetics of petroleum
750 generation and cracking by programmed-temperature closed-system pyrolysis of
751 Toarcian Shales. Fuel 77, 23–31.

752 Dominé, F., 1989. Kinetics of hexane pyrolysis at very high pressures. 1. Experimental
753 study. Energy & Fuels 3, 89–96.

754 Dominé, F., 1991. High pressure pyrolysis *n*-hexane, 2-4 dimethylpentane and 1-
755 phenylbutane. Is pressure an important geochemical parameter? Organic
756 Geochemistry 17, 619–634.

757 Dominé, F., Dessort, D., Brevart, O., 1998. Towards a new method of geochemical
758 kinetic modelling: Implications for the stability of crude oils. Organic
759 Geochemistry 28, 597–612.

760 Dominé, F., Marquaire, P.M., Muller, C., Côme, G.M., 1990. Kinetics of hexane
761 pyrolysis at very high pressures. 2. Computer modeling. Energy & Fuels, 4, 2–
762 10.

763 Fabuss, B.M., Smith, J.O., Satterfield, C.N., 1964. Thermal cracking of pure saturated
764 hydrocarbons. In: McKetta, J. (Ed.), Advances in Petroleum Industry and
765 Refining. Wiley and Sons, pp. 156–201.

766 Ford, T.J., 1986. Liquid-Phase thermal decomposition of hexadecane: reaction
767 mechanisms. Industrial and Engineering Chemistry Fundamentals 25, 240–243.

768 Freund, H., Olsmtead, W.N., 1989. Detailed chemical kinetic modelling of
769 butylbenzene pyrolysis. International Journal of Chemical Kinetics 21, 561–574.

770 Hayes, J.M., 1991. Stability of petroleum. Nature 252, 108–109.

771 Hesp, W. Rigby, D., 1973. The geochemical alteration of hydrocarbons in the presence
772 of water. Erdol Kohle - Erdgas 26, 70–76.

773 Hill, R.J., Tang, Y., Kaplan, I.R., Jenden, P.D., 1996. The influence of pressure on the
774 thermal cracking of oil. Energy & Fuels 10, 873–882.

775 Hill, R.J., Tang, Y., Kaplan, I.R., 2003. Insights into oil cracking based on laboratory
776 experiments. Organic Geochemistry 34, 1651–1672.

777 Hoering, T. C., 1984. Thermal reactions of kerogen with added water, heavy water and
778 pure organic substances. Organic Geochemistry 5, 267–278.

779 Jackson, K.J., Burnham, A.K., Braun, R.L., Knauss, K.G., 1995. Temperature and
780 pressure dependence of *n*-hexadecane cracking. Organic Geochemistry 23, 941–
781 953.

782 Jones, D.M., Douglas, A.G., Connan, J., 1988. Hydrous pyrolysis of asphaltenes and
783 polar fractions of biodegraded oils. Organic Geochemistry 13, 981–993.

784 Khorasheh, F., Gray, M.R., 1993a. High-pressure thermal cracking of *n*-hexadecane.
785 Industrial and Engineering Chemistry Research 32, 1853–1863.

786 Khorasheh, F., Gray, M.R., 1993b. High-pressure thermal cracking of *n*-hexadecane in
787 aromatic solvents. Industrial and Engineering Chemistry Research 32, 1864–
788 1876.

789 Kuangzong, Q., Qiushui, Y., Shaohui, G., Qinghua, L., Wei, S., 1994. Chemical
790 structure and hydrocarbon formation of the Huanxian brown coal, China.
791 Organic Geochemistry 21, 333-341.

792 Lannuzel, F., Bounaceur, R., Michels, R., Scacchi, G., Marquaire, P-M., 2010.
793 Reassessment of the kinetic influence of toluene on *n*-alkanes pyrolysis. Energy
794 & Fuels 24, 3817–3830.

795 Lehne, E., Dieckmann, V., 2007a. Bulk kinetic parameters and structural moieties of
796 asphaltenes and kerogens from a sulphur-rich source rock sequence and related
797 petroleums. Organic Geochemistry 38, 1657–1679.

798 Lehne, E., Dieckmann, V., 2007b. The significance of kinetic parameters and structural
799 markers in source rock asphaltenes, reservoir asphaltenes and related source
800 rock kerogens, the Duvernay Formation (WCSB). Fuel 86, 887–901.

801 Leininger, J.P., Lorant, F., Minot, C., Behar, F., 2006. Mechanism of 1-
802 methylnaphthalene pyrolysis in a batch reactor and relevance with other
803 methylated polyaromatics. Energy & Fuels 20, 2518–2530.

804 Lewan, M. D., 1997. Experiments on the role of water in petroleum formation.
805 Geochimica et Cosmochimica Acta 61, 3691-3723.

806 Lewan, M.D., Ruble, T.E., 2002. Comparison of petroleum generation kinetics by
807 isothermal hydrous and nonisothermal open-system pyrolysis. Organic
808 Geochemistry 33, 1457–1475.

809 Mango, F.D., 1991. The stability of hydrocarbons under the time-temperature
810 conditions of petroleum genesis. Nature 352, 146–148.

811 McKinney, D.E., Behar, F., Hatcher, P.G., 1998. Reaction kinetics and *n*-alkane product
812 profiles from the thermal degradation of ^{13}C-labeled *n*-C_{25} in two dissimilar oils
813 as determined by SIM/GC/MS. Organic Geochemistry. 29, 119–136.

814 Michels, R., Landais, P., 1994. Artificial coalification: Comparison of confined
815 pyrolysis and hydrous pyrolysis. Fuel 73, 1691-1696.

816 Michels, R., Landais, P., Philp, R.P., Torkelson, B., 1995. Influence of pressure and the
817 presence of water on the evolution of the residual kerogen during confined,
818 hydrous, and high-pressure hydrous pyrolysis of Woodford Shale. Energy &
819 Fuels. 9, 204–215.

820 Michels, R., Lannuzel, F., Bounaceur, R., Burklé-Vitzthum,V., Marquaire, P-M., 2015.
821 Quantitative modelling of the effects of pressure on hydrocarbon cracking
822 kinetics in experimental and petroleum reservoir conditions. In: Francu, J.,
823 Schwark, L., Ocásková, D., Čáslavský, J., Brejchová, D. (Eds). Proceedings of
824 the 27th International Meeting on Organic Geochemistry, Prague, 13-18th
825 September, 2005, Abstract D0512.

826 Murray, I.P., Love, G.D., Snape, C.E., Bailey, N.J.L., 1998. Comparison of covalently-
827 bound aliphatic biomarkers released via hydropyrolysis with their solvent-
828 extractable counterparts for a suite of Kimmeridge clays. Organic Geochemistry
829 29, 1487–1505.

Panfilova, I., Michels, R., Bounaceur, R., Burklé-Vitzthum,V., Serres, M., Jamilyam Ismailova1, J., Marquaire, P-M., 2015. Thermal stability of hydrocarbons in geological reservoir: coupling chemical kinetics and transport in porous media models. In: Francu, J., Schwark, L., Ocásková, D., Čáslavský, J., Brejchová, D. (Eds). Proceedings of the 27th International Meeting on Organic Geochemistry, Prague, 13-18th September, 2005, Abstract D0513.

Poutsma, M.L., 1990. Free-radical thermolysis and hydrogenolysis of model hydrocarbons relevant to processing of coal. Energy & Fuels 4, 113–131.

Price, L.C., 1982. Organic geochemistry of core samples from an ultra-deep well (300 °C, 7 km). Chemical Geology 37, 215–228.

Price, L.C., 1990. Crude-oil characterisation at Caillou Island, Louisiana by "genetic" hydrocarbons. In: Schumacher, D.G., Perkins, B.F. (Eds.), Gulf Coast Oils and Gases: Their Characteristics, Origin, Distribution and Exploration and Production Significance. SEPM, 237–261.

Price, L.C., Clayton, J.L., Rumen, L.L., 1979. Organic geochemistry of a 6.9 km deep well, Hinds County, Mississippi. Gulf Coast Association and Geologic Society Transcripts 29, 352–370.

Price, L.C., Clayton, J.L., Rumen, L.L., 1981. Organic geochemistry of the 9.6 km Bertha Rogers #1, Oklahoma. Organic Geochemistry 3, 59–77.

Rice, F.O., 1931. The thermal decomposition of organic compounds from the standpoint of free radicals. I- Saturated hydrocarbons. Journal of American Chemical Society 53, 1959–1972.

852 Rice, F.O., 1933. The thermal decomposition of organic compounds from the standpoint
853 of free radicals. III. The calculations of the products formed from paraffin
854 hydrocarbons. Journal of American Chemical Society 55, 3035–3040.

855 Rice, F.O., Herzfeld, K.F., 1934. The thermal decomposition of organic compounds
856 from the standpoint of free radicals. VI. The mechanism of some chain
857 reactions. Journal of the American Chemical Society 56, 284–289.

858 Russell, C.A., Snape, C.E., Meredith, W., Love, G.D., Clarke, Ed., Moffatt, B., 2004.
859 The potential of bound biomarker profiles released via catalytic hydropyrolysis
860 to reconstruct basin charging history for oils. Organic Geochemistry 35, 1441–
861 1459.

862 Savage, P.E., Klein, M.T., 1987. Asphaltene reaction pathways. 2. Pyrolysis of *n*-
863 pentadecylbenzene. Industrial and Engineering Chemistry Research 26, 488–
864 494.

865 Schenk, H. J., Di Primio, R., Horsfield, B., 1997. The conversion of oil into gas in
866 petroleum reservoirs. Part I: Comparative kinetic investigation of gas generation
867 from crude oils of lacustrine, marine and fluviodeltaic origin by programmed
868 temperature closed-system pyrolysis. Organic Geochemistry 26, 467–481.

869 Scotchman, I.C., Meredith, W., Snape, C.E., Carr, A.D., 2006. The use of bitumens as a
870 valuable tool for the timing of charge in basin modelling. Abstract. American
871 Association of Petroleum Geologist meeting, Perth Australia.

872 Smith, C.M., Savage, P.E., 1991. Reactions of polycyclic alkylaromatics: Structure and
873 reactivity. American Institute of Chemical Engineers Journal 37, 1613–1624.

874 Smith, C.M., Savage, P.E., 1994. Reactions of polycyclic alkylaromatics. 6. Detailed
875 chemical kinetic modelling. Chemical Engineering Science 49, 259–270.

876 Sofer, Z., 1988. Hydrous pyrolysis of Monterey asphaltenes. Organic Geochemistry 13,
877 939–945.

878 Solli, H., Leplat, P., 1986. Pyrolysis-gas chromatography of asphaltenes and kerogens
879 from source rocks and coals-A comparative structural study. Organic
880 Geochemistry 10, 313–329.

881 Song, C., Lai, W., Schobert, H.H., 1994. Condensed-phase pyrolysis of the *n*-
882 tetradecane at elevated pressures for long duration. Products and reaction
883 mechanism. Industrial and Engineering Chemistry Research 33, 534–547.

884 Tissot, B.P., Welte, D.H., 1984. Petroleum formation and occurrence. Springer-Verlag,
885 Berlin.

886 Tsuzuki, N., Takeda, N., Suzuki, M., Yokoi, K., 1999. The kinetic modelling of oil
887 cracking by hydrothermal pyrolysis experiments. International Journal of Coal
888 Geology 39, 227–250.

889 Uguna, C.N., Carr, A.D., Snape, C.E., Meredith, W., Castro-Díaz, M., 2012a. A
890 laboratory pyrolysis study to investigate the effect of water pressure on
891 hydrocarbon generation and maturation of coals in geological basins. Organic
892 Geochemistry 52, 103–113.

893 Uguna, C.N., Snape, C.E., Meredith, W., Carr, A.D., Scotchman, I.C., Davis, R.C.,
894 2012b. Retardation of hydrocarbon generation and maturation by water pressure

in geological basins: an experimental investigation. In: Peters, K.E., Curry, D.J., Kacewicz, M. (Eds.), Basin Modelling: New Horizons in Research and Applications: AAPG Hedberg Series, No. 4, 19–37.

Uguna, C.N., Azri, M.H., Snape, C.E., Meredith, W., Carr, A.D., 2013. A hydrous pyrolysis study to ascertain how gas yields and the extent of maturation for partially matured source rock and bitumen in isolation compared to their whole source rock. Journal of Analytical and Applied Pyrolysis 103, 268–277.

Uguna, C.N., Carr, A.D., Snape, C.E., Meredith, W., 2015. High pressure water pyrolysis of coal to evaluate the role of pressure on hydrocarbon generation and source rock maturation at high maturities under geological conditions. Organic Geochemistry 78, 44–51.

Uguna, C.N., Carr, A.D., Snape, C.E., Meredith, W., Scotchman, I.C., Murray, A., Vane, C.H., 2016. Impact of high water pressure on oil generation and maturation in Kimmeridge Clay and Monterey source rocks: Implication for petroleum retention and gas generation in shale gas systems. Journal of Marine and Petroleum Geology 73, 72-85.

Ungerer, P., Behar, F., Villalba, M., Heum, O.R., Audibert, A., 1988. Kinetic modelling of oil cracking. Organic Geochemistry 13, 857–868.

Ungerer, P., Pelet, R., 1987. Extrapolation of the kinetics of oil and gas formation from laboratory experiments to sedimentary basins. Nature 327, 52–54.

915 Vandenbroucke, M., Behar, F., Rudkiewicz, J.L., 1999. Kinetic modelling of petroleum
916 formation and cracking: implications from the high pressure/high temperature
917 Elgin Field (UK, North Sea). Organic Geochemistry 30, 1105–1125.

918 Voge, H.H., Good, G.M., 1949. Thermal cracking of higher paraffins. Journal of
919 American Chemical Society 71, 593–597.

920 Wilhelms, A., Larter, S.R., 1995. Overview of the geochemistry of some tar mats from
921 the North Sea and USA: implications for tar-mat origin. In: Cubitt, J.M.,
922 England, W.A. (Eds.), the Geochemistry of Reservoirs. Geological Society,
923 London, Special Publications 86, 87–101.

924 Wu, G., Katsumura, Y., Matsuura, C., Ishigure, K., 1996. Comparison of liquid-phase
925 and gas-phase thermal cracking of *n*-hexadecane. Industrial and Engineering
926 Chemistry Research 35, 4747–4754.

927 Yu, J., Eser, S., 1998. Thermal decomposition of jet fuel compounds under-near critical
928 and supercritical conditions. 2. Decalin and tetralin. Industrial and Engineering
929 Chemistry Research 37, 4601–4608.

930 Zhou, P., Hollis, O.L., Crynes, B.L., 1987. Thermolysis of higher molecular weight
931 straight-chain alkanes. Industrial and Engineering Chemistry Research 26, 846–
932 852.

933

934

935

936 **Figure captions**

937 Fig. 1. Schematic diagram of pyrolysis equipment.

938

939 Fig. 2. Flow chart showing pyrolysis conditions, products recovery and analysis.

940

941 Fig. 3. (a) GC profiles of the initial and pyrolysed oils, (b) GC profiles of 175 and 900
942 bar oils [normalised to abundance of methylcyclohexane (MCH)] comparing extent of
943 UCM under both conditions.

944

945 Fig. 4. (a) GC-MS total ion chromatograms profiles for the cracked *n*-hexadecane under
946 non-hydrous (20 bar) , 175 bar, 500 bar and 900 bar conditions, (b) Expanded GC-MS
947 total ion chromatograms for C_{18}-C_{31} hydrocarbons from *n*-hexadecane cracking under
948 non-hydrous (20 bar), 175 bar, 500 bar and 900 bar.

949

950 Fig. 5. Toluene to C_7 *n*-alkane, methylcyclohexane to C_7 *n*-alkane, and short to long
951 chain *n*-alkane peak area ratios for initial and pyrolysed oils.

952

953 Fig. 6. Short and long chain *n*-alkane ratios of initial to pyrolysed oil with increase in
954 pressure.

955

956 Fig. 7. (a) GC profile for Gulf of Mexico bitumen whole oil, (b) Gulf of Mexico
957 bitumen free sterane biomarker GC-MS trace, (c) Gulf of Mexico bitumen asphaltene
958 bound sterane biomarker GC-MS trace.

959

960 Table 1. Hydrocarbon gas yields (mg/g carbon) for the oil and *n*-hexadecane.

961

Oseberg oil Samples	CH_4	C_2H_4	C_2H_6	C_3H_6	C_3H_8	C_4 alkenes	C_4 alkanes	C_5 alkenes	C_5 alkanes	Total C_1-C_5
Non-hydrous (20 bar)	0.86	0.07	0.62	0.26	0.68	0.18	0.78	0.08	1.77	5.30
175 bar	0.35	0.02	0.15	0.03	0.25	0.01	0.74	0.00	1.41	2.95
500 bar	0.07	0.00	0.03	0.00	0.23	0.01	0.85	0.00	1.27	2.45
900 bar	0.07	0.00	0.02	0.00	0.14	0.01	0.63	0.00	1.02	1.89
n-hexadecane samples	CH_4	C_2H_4	C_2H_6	C_3H_6	C_3H_8	C_4H_{10}				Total C_1-C_4
Non-hydrous (20 bar)	0.55	0.04	0.36	0.31	0.37	0.22				1.85
175 bar	0.08	0.02	0.20	0.09	0.18	0.07				0.65
500 bar	0.01	0.00	0.01	<0.01	0.01	0.01				0.04
900 bar	0.01	0.00	0.01	<0.01	0.01	0.01				0.04

962
963
964
965
966
967
968
969
970
971
972
973
974
975
976
977
978
979
980 Fig. 1
981

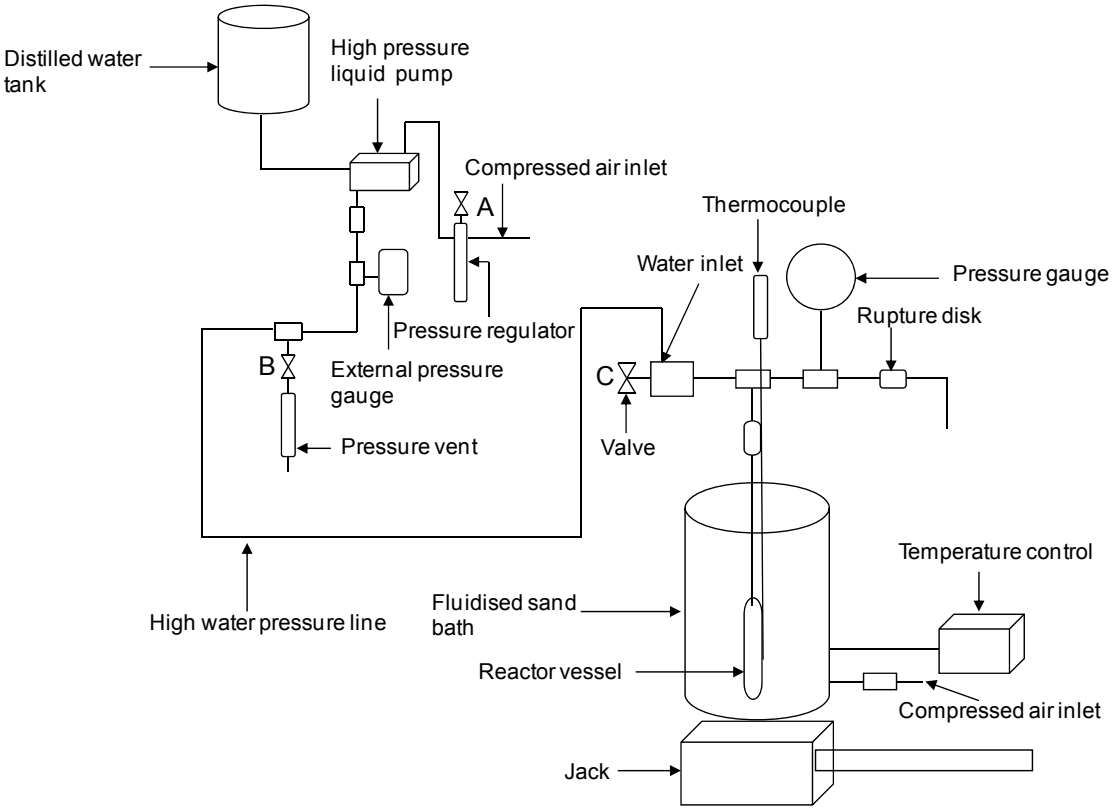
Distilled water tank
High pressure liquid pump
Compressed air inlet
A
Thermocouple
Water inlet
Pressure gauge
Rupture disk
Pressure regulator
B
External pressure gauge
C
Valve
Pressure vent
Temperature control
Fluidised sand bath
High water pressure line
Reactor vessel
Compressed air inlet
Jack

1009 Fig. 2
1010
1011

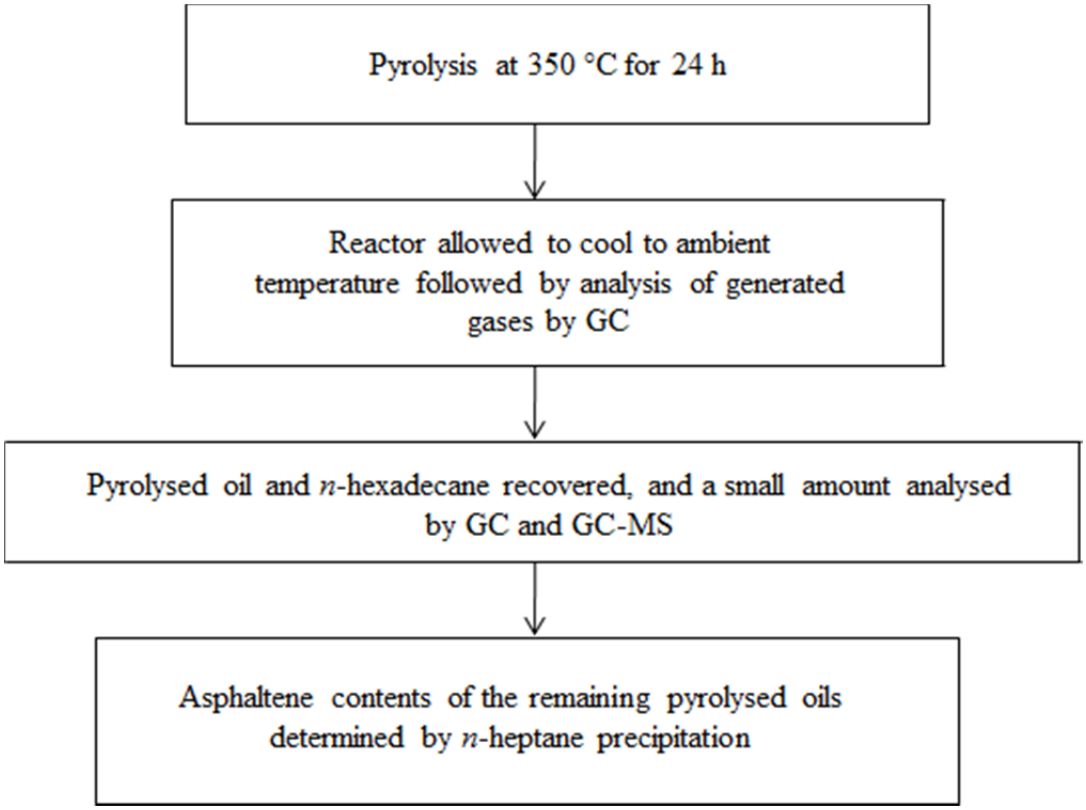

1012
1013

1014 Fig. 3a
1015

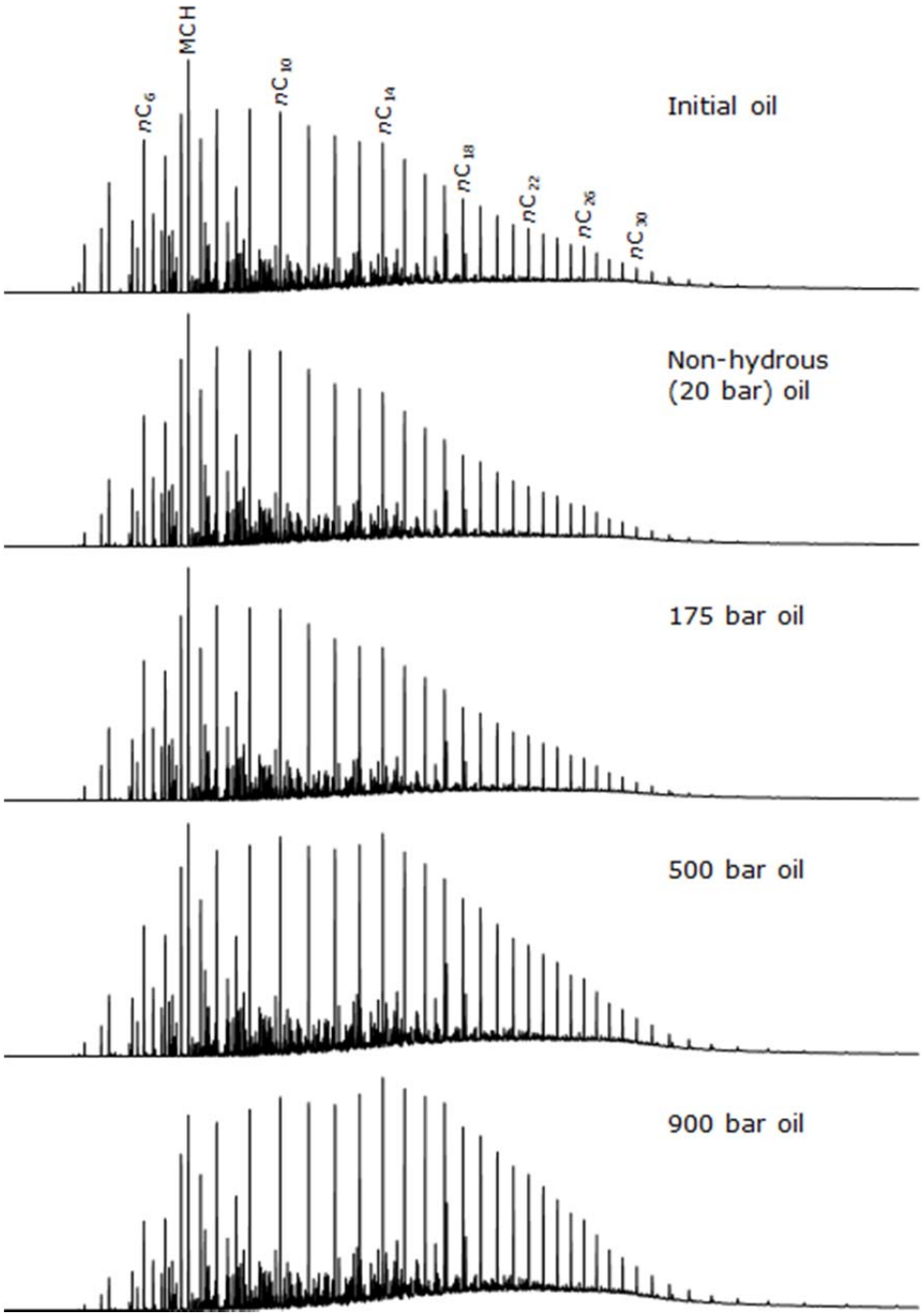

1016
1017

1018

1019 Fig. 3b

1020

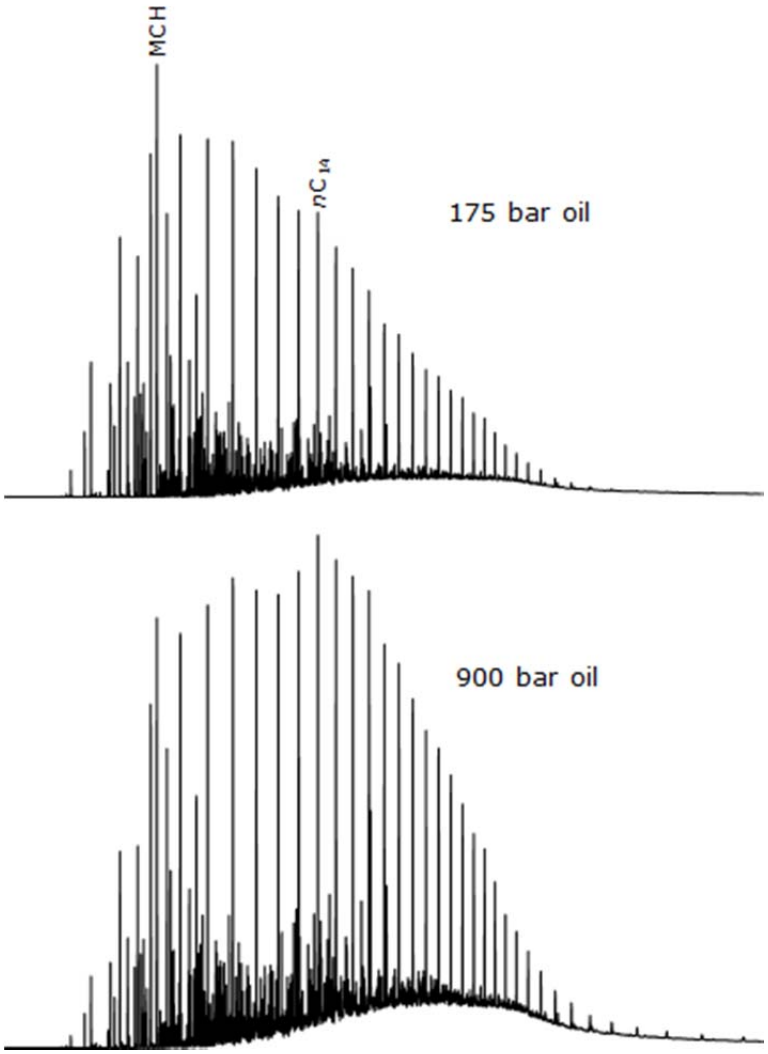

1021

1022

1023

1024 Fig. 4a

1025

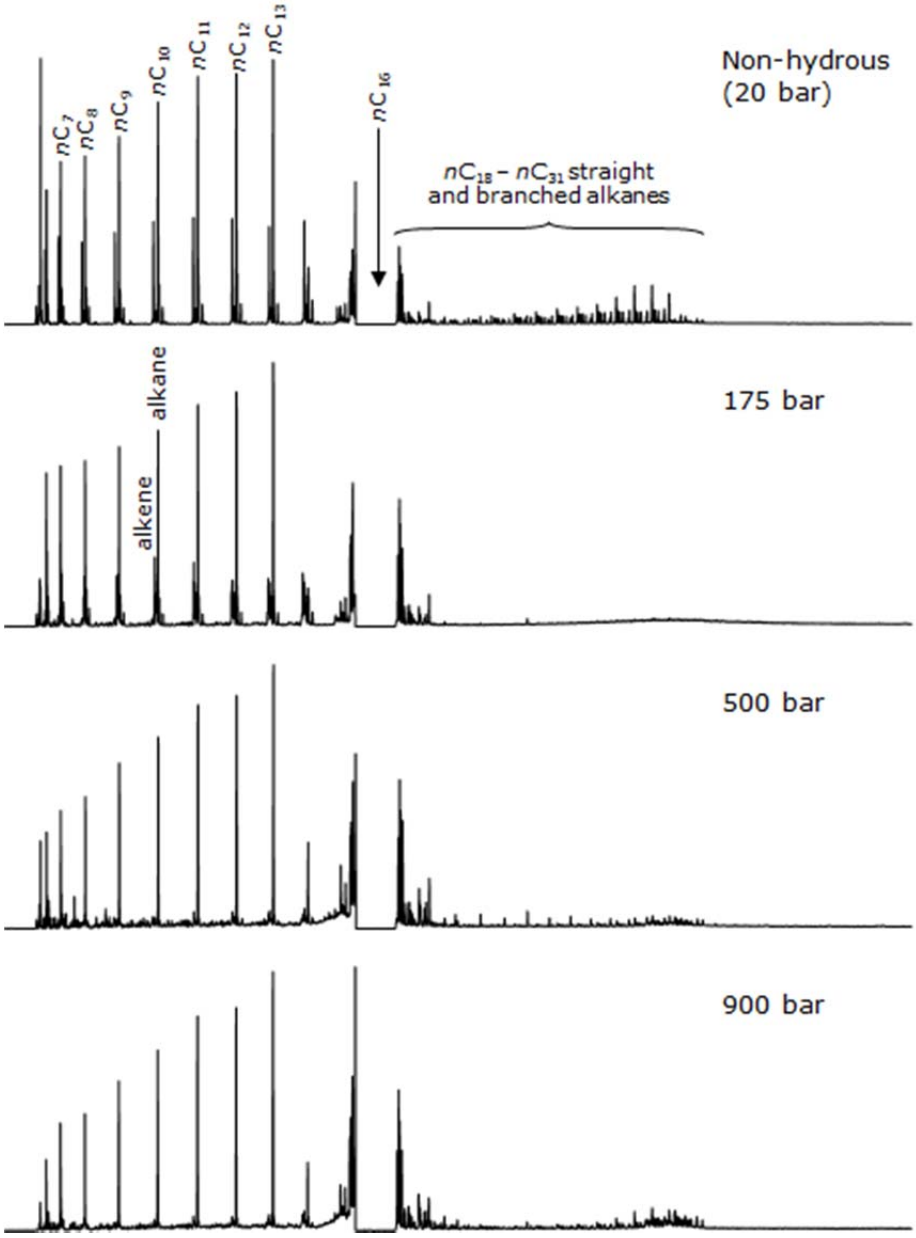

1026

1027

1028

1029 Fig. 4b

1030

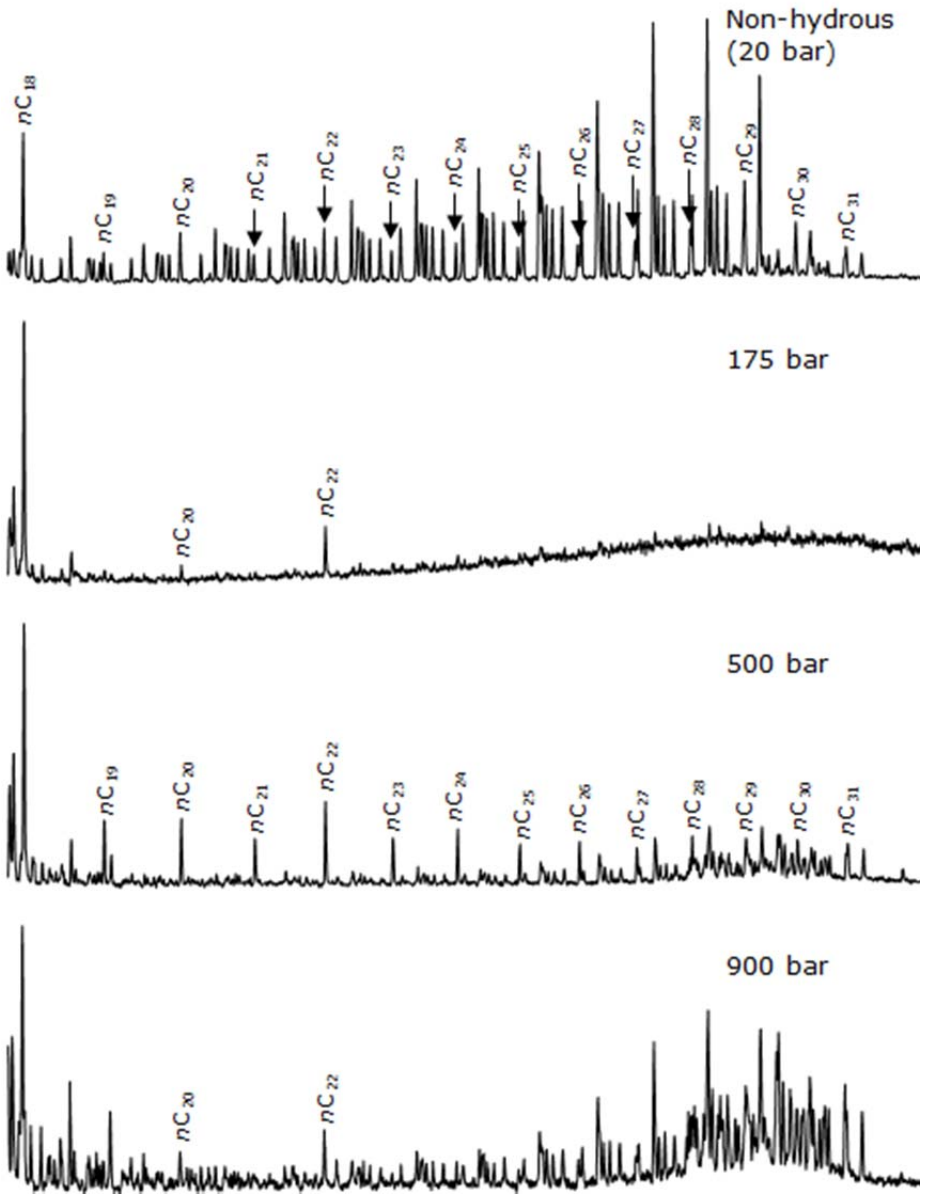

1031

1032

1033

1034 Fig. 5

1035

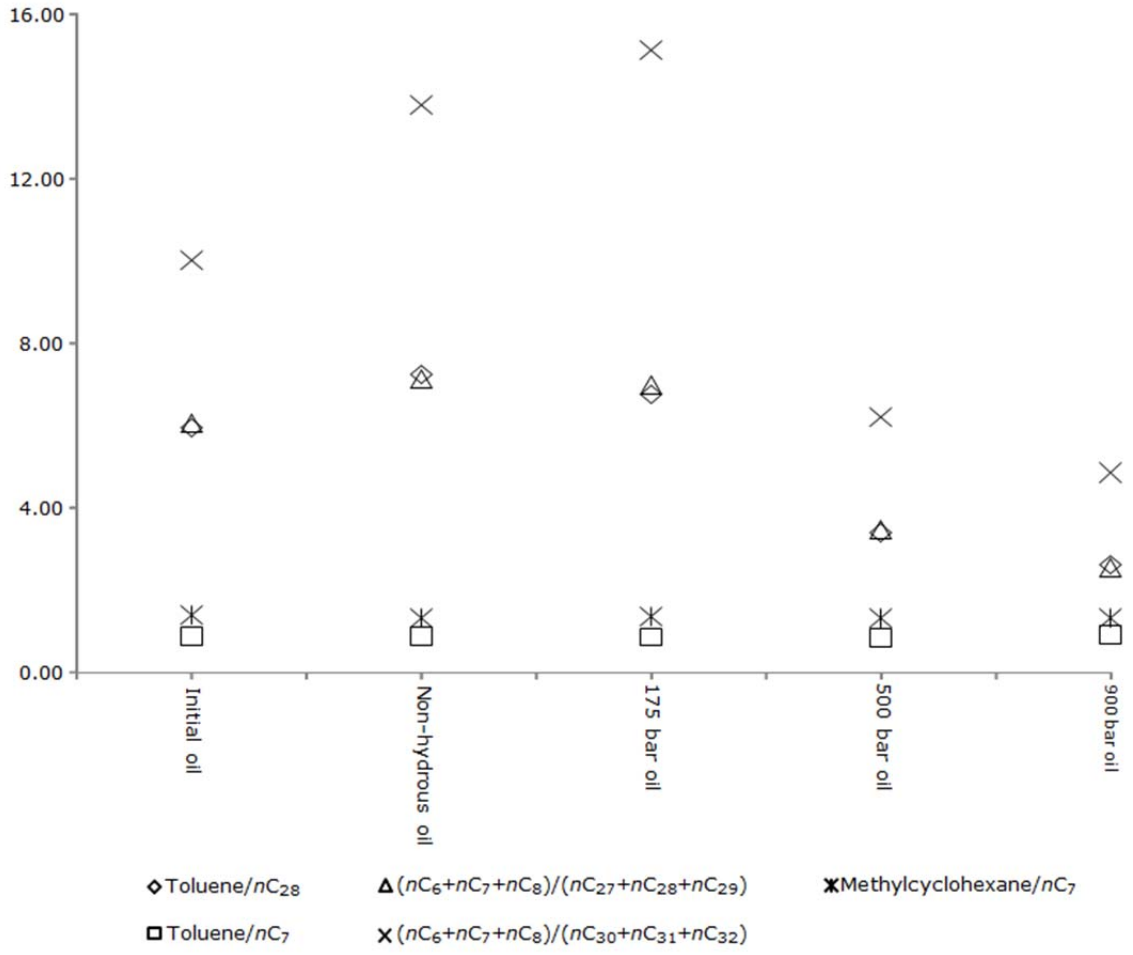

1036

1037

1038

1039 Fig. 6

1040

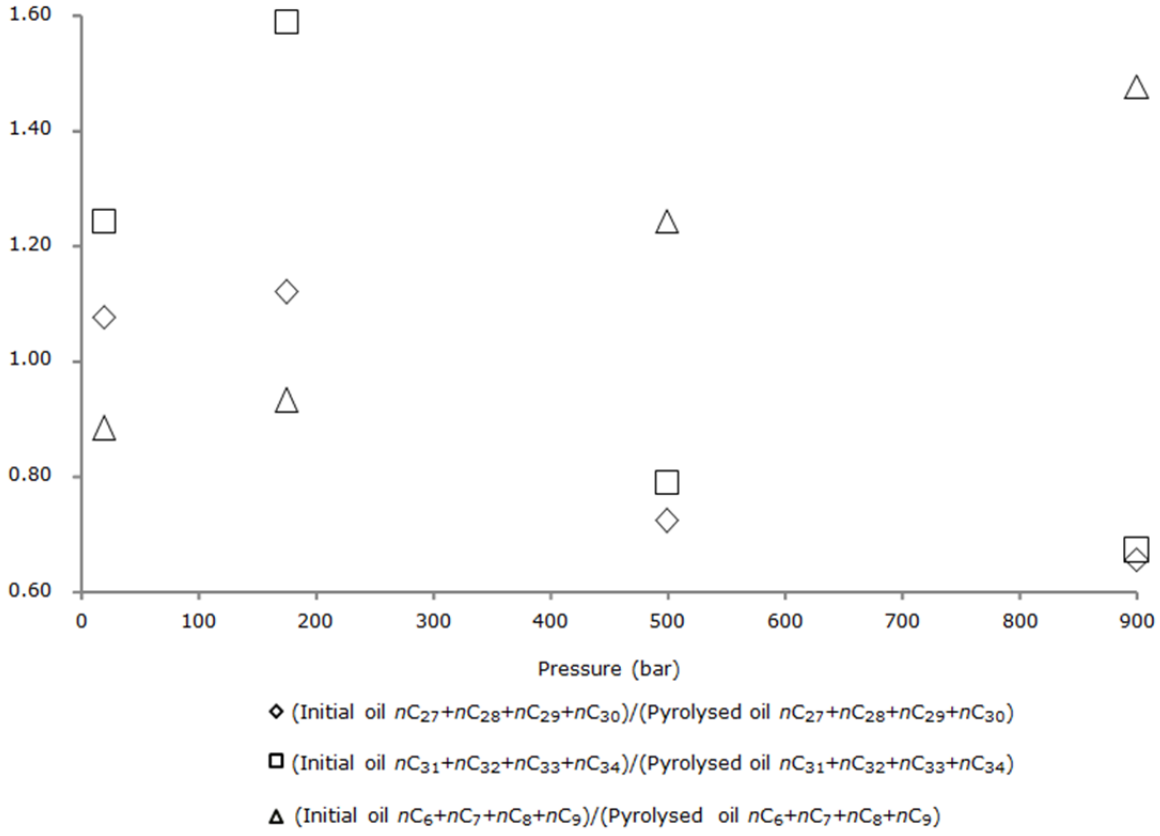

1041

1042

1043

1044
1045 Fig. 7a

1046

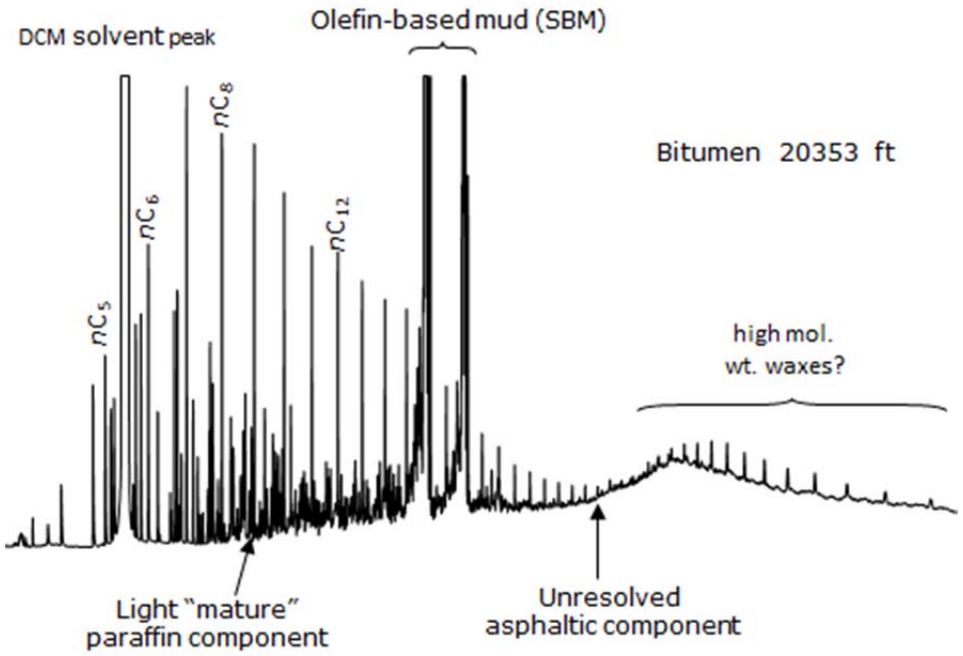

1047

1048

1049

1050 Fig. 7b

1051

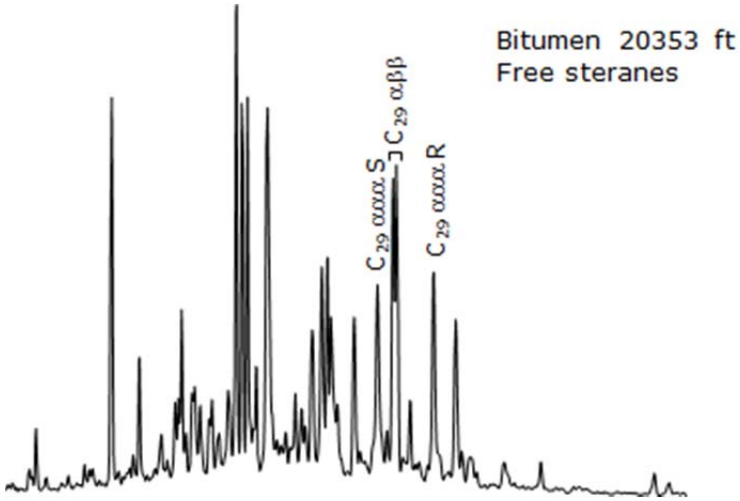

1052

1053

1054

1055 Fig. 7c

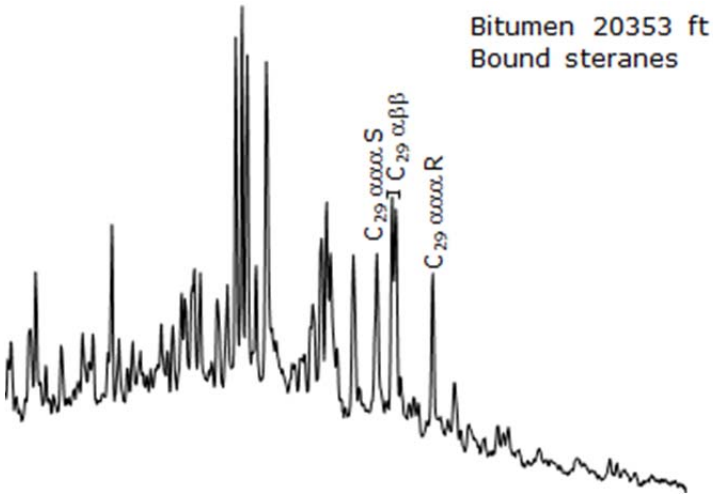

1056

1057

1058

1059